Galectin-9 controls the therapeutic activity of 4-1BB–targeting antibodies

Shravan Madireddi,[1] So-Young Eun,[1] Seung-Woo Lee,[1] Ivana Nemčovičová,[2] Amit Kumar Mehta,[1] Dirk M. Zajonc,[2] Nozomu Nishi,[3] Toshiro Niki,[4,5] Mitsuomi Hirashima,[4,5] and Michael Croft[1]

[1]Division of Immune Regulation and [2]Division of Cell Biology, La Jolla Institute for Allergy and Immunology, La Jolla, CA 92037
[3]Life Science Research Center; and [4]Department of Immunology and Immunopathology, Faculty of Medicine; Kagawa University, Kagawa 761-0793, Japan
[5]GalPharma Co., Ltd., Kagawa 760-0301, Japan

Biologics to TNF family receptors are prime candidates for therapy of immune disease. Whereas recent studies have highlighted a requirement for Fcγ receptors in enabling the activity of CD40, TRAILR, and GITR when engaged by antibodies, other TNFR molecules may be controlled by additional mechanisms. Antibodies to 4-1BB (CD137) are currently in clinical trials and can both augment immunity in cancer and promote regulatory T cells that inhibit autoimmune disease. We found that the action of agonist anti–4-1BB in suppressing autoimmune and allergic inflammation was completely dependent on Galectin-9 (Gal-9). Gal-9 directly bound to 4-1BB, in a site distinct from the binding site of antibodies and the natural ligand of 4-1BB, and Gal-9 facilitated 4-1BB aggregation, signaling, and functional activity in T cells, dendritic cells, and natural killer cells. Conservation of the Gal-9 interaction in humans has important implications for effective clinical targeting of 4-1BB and possibly other TNFR superfamily molecules.

CORRESPONDENCE
Michael Croft:
mick@liai.org

Abbreviations used: BAL, bronchoalveolar lavage; CRD, cysteine-rich domain; EAE, experimental autoimmune encephalomyelitis; PFA, paraformaldehyde; PLAD, preligand assembly domain; RALDH, retinal dehydrogenase; SPR, surface plasmon resonance.

Protein receptors on immune cells are major targets for clinical intervention in autoimmune disease and cancer, leading to the development of biologics that either agonize or antagonize these molecules. In particular, the TNF/TNFR superfamily has become the subject of intense interest given the success of TNF blockers in several inflammatory indications (Croft et al., 2013). In the area of agonist therapy, major targets in the TNFR superfamily are molecules such as CD40, OX40, GITR, TRAILR, and 4-1BB, with the goal of stimulating these receptors to either promote effector T and NK cell activity in cancer or promote the generation of regulatory T cells in autoimmunity, or in the case of TRAILR to directly induce death in tumor cells (Croft et al., 2013). As such, recent efforts have focused on understanding how agonist antibodies exert their stimulating activity. In most cases, it is thought that TNFR family molecules are naturally stimulated by trimeric ligands, leading to the notion that at least three TNFR monomers might need to be engaged for effective signaling to result. Whether this is the case is not clear as many bivalent agonist antibodies, which theoretically bind only two TNFR family monomers, are highly functional when soluble. Interestingly, several studies over the past few years have found a requirement for either stimulatory or inhibitory Fcγ receptors for the therapeutic activity of agonist antibodies to TRAILR, CD40, and GITR (Nagae et al., 2006; Wilson et al., 2011; Bulliard et al., 2013). This implies that Fc receptors may promote aggregation of TNFR family monomers, although elicitation of other molecular or cellular activities cannot be ruled out. However, not all agonist antibodies to TNFR family molecules appear to need Fc receptors for their activity, either implying receptor trimerization or aggregation is not required or that other mechanisms

S. Madireddi and S.-Y. Eun contributed equally to this paper.
S.-W. Lee's present address is Lab of Immune Regulation, Division of Integrative Biosciences and Biotechnology, Pohang University of Science and Technology, Pohang, Gyungbuk 790-784, South Korea.
I. Nemčovičová's present address is Dept. of Molecular Medicine, Institute of Virology, Slovak Academy of Sciences, 84505 Bratislava, Slovakia.

The Rockefeller University Press $30.00
J. Exp. Med. 2014 Vol. 211 No. 7 1433-1448
www.jem.org/cgi/doi/10.1084/jem.20132687

The Journal of Experimental Medicine

may exist to promote clustering of receptors into functional signaling units.

4-1BB (CD137, TNFRSF9) is a cysteine-rich cell surface molecule that is inducible on a variety of immune cells including T cells, NK cells, and DCs, and the interaction with its TNF family ligand, 4-1BBL, controls natural immunity to viruses (Salek-Ardakani and Croft, 2010; Snell et al., 2011). 4-1BB is also of great clinical interest in that agonist reagents to this molecule can exert two divergent activities, both promoting immune responses against tumors and viruses and inducing immunoregulatory activity that suppresses symptoms in multiple models of autoimmune and inflammatory disease (Watts, 2005; So et al., 2008). Several antibodies to 4-1BB are currently in clinical trials for cancer (Ascierto et al., 2010; Vinay and Kwon, 2012; Croft et al., 2013), and therefore the molecular mechanisms by which the activity of 4-1BB is controlled are of strong biological and therapeutic importance.

Here, we identify Galectin-9 (Gal-9), a member of the β-galactoside–binding family of lectins, as critical for the functional activities of antibodies to 4-1BB in controlling immune disease in vivo. The Galectins are carbohydrate-binding proteins, containing homologous carbohydrate recognition domains, and can play important roles in regulating immune cell homeostasis and inflammation (Rabinovich and Toscano, 2009). Gal-9 can be highly modulatory for immune function depending on the circumstance (Wiersma et al., 2013), and at least some of this activity is thought to be mediated by the inhibitory molecule T cell immunoglobulin mucin 3 (Tim-3), which was previously described to bind to Gal-9 (Zhu et al., 2005). We found that in models of experimental autoimmune encephalomyelitis (EAE) and asthma, in which an agonist antibody of 4-1BB suppresses disease, that the protective effect was lost in mice that lacked Gal-9. Experiments in vitro showed that the stimulatory function of anti–4-1BB in T cells, DCs, and NK cells was impaired when Gal-9 was absent. The extracellular portion of 4-1BB comprises four cysteine-rich or TNFR motifs, and it has several potential N-linked glycosylation sites. Surface plasmon resonance (SPR) and biochemical analyses demonstrated that human and mouse 4-1BB bound to human and mouse Gal-9 with high affinity, in a carbohydrate-dependent manner, largely via the fourth, most cell membrane–proximal, cysteine-rich domain (CRD). This did not overlap with the agonist antibody-binding sites in 4-1BB or the binding site for the natural ligand of 4-1BB, suggesting that Gal-9 facilitates the clustering of 4-1BB molecules when engaged by agonist antibodies or its ligand. The interaction of Gal-9 with 4-1BB is then a previously unknown immunoregulatory checkpoint, which may be exploited in the future development of biologics to modify immune disease.

RESULTS

Anti–4-1BB is unable to ameliorate inflammatory disease in mice deficient in Gal-9

Numerous studies have shown that administration of agonist anti–4-1BB can strongly suppress clinical symptoms in mouse models ranging from collagen-induced arthritis (Seo et al., 2004) to experimental autoimmune uveoretinitis (Choi et al., 2006), EAE (Sun et al., 2002; Kim et al., 2011), systemic lupus erythematosus (Foell et al., 2003), and asthma (Polte et al., 2006). However, the requirements for the activity of anti–4-1BB are largely unknown. We reasoned that immunosuppressive molecules might be involved, and Gal-9 was one candidate based on data describing Gal-9 as a ligand for the inhibitory molecule Tim-3, and that administration of Gal-9 can suppress disease in many of the same scenarios in which anti–4-1BB was inhibitory (Zhu et al., 2005; Wiersma et al., 2013).

We initially used a model of EAE driven by $MOG_{33–55}$ peptide and chose this because endogenous 4-1BB interactions do not play any role in development of disease (unpublished data). We tested the ability of anti–4-1BB to suppress demyelinating disease when injected at the time of immunization. As reported previously (Sun et al., 2002; Kim et al., 2011), anti–4-1BB strongly blocked the clinical symptoms of disease in WT mice. Gal-$9^{-/-}$ mice developed EAE similarly to WT mice based on clinical scoring, showing there is no intrinsic defect in mounting this response when Gal-9 was not expressed. However, quite strikingly, anti–4-1BB was unable to suppress disease in Gal-$9^{-/-}$ mice (Fig. 1 a). Hematoxylin and eosin (H&E) staining of spinal cords further showed that anti–4-1BB injection did not suppress cellular infiltration in Gal-$9^{-/-}$ mice as it did in WT mice (Fig. 1 b). Intracellular staining for IL-17A in CD4 T cells from draining LNs also revealed a suppressed Th17 response in WT mice that received anti–4-1BB, but not in Gal-$9^{-/-}$ mice (Fig. 1 c).

The primary mechanism that has been proposed to explain the immunosuppressive activity of agonists to 4-1BB is through expansion of a regulatory population of CD8 T cells that express CD11c and can block the induction of autoreactive or inflammatory CD4 T cells, associated with producing high levels of IFN-γ (Seo et al., 2004; Choi et al., 2006; Kim et al., 2011). We then assessed the induction of this population of T cells in the draining LNs of MOG-immunized mice. Anti–4-1BB induced a significant expansion of $CD8^+CD11c^+$ T cells that made extremely high amounts of IFN-γ in WT mice, but their accumulation was impaired in Gal-$9^{-/-}$ mice (Fig. 1, d–f).

We further investigated the suppressive ability of anti–4-1BB in an allergic asthma model. Administration of anti–4-1BB at the time of immunization with antigen almost completely prevented airway inflammation in WT mice, as shown by histological evaluation of lung sections, and eosinophilia in the bronchoalveolar lavage (BAL) fluid (Fig. 2, a and b). This was accompanied by a decreased antigen-specific recall T cell response and a switch from IL-5 to IFN-γ production (Fig. 2 c). In contrast, anti–4-1BB had almost no detectable activity in Gal-$9^{-/-}$ mice (Fig. 2, a–c). Again, analysis of $CD8^+CD11c^+$ T cells making IFN-γ showed that anti–4-1BB significantly expanded this population in WT mice but not in Gal-$9^{-/-}$ mice (Fig. 2, d and e). Collectively, these data show that the immunomodulatory activity of anti–4-1BB in vivo is dependent on Gal-9.

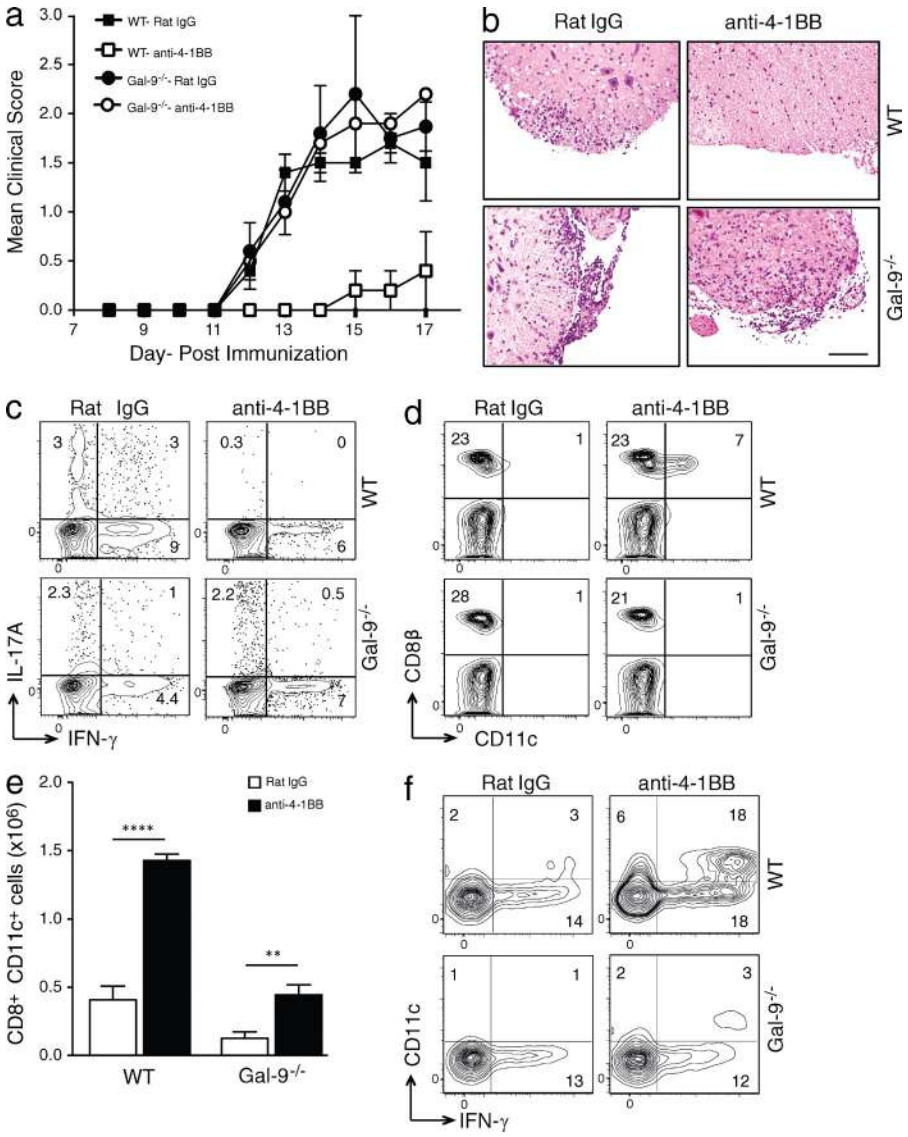

Figure 1. Gal-9 is required for suppression of EAE by anti–4-1BB in vivo. (a and b) Mean clinical score (a) and H&E staining of spinal cords isolated on day 18 (b) from WT or Gal-9$^{-/-}$ mice that were immunized with MOG_{35-55} peptide and injected with either control rat Ig or agonist anti–4-1BB. Data are means ± SEM from five mice per group. Similar results were seen in four different experiments. Bar, 200 µm. (c) Intracellular IL-17A and IFN-γ expression in draining LN CD4$^+$ T cells on day 18 after in vitro restimulation with 200 µg/ml MOG_{35-55} peptide for 72 h. (d and e) Proportion (d) and absolute number (e) of gated CD3$^+$ cells in draining LNs at day 18 expressing CD8β and CD11c. Data are mean ± SEM from five mice per group. **, $P < 0.01$; ****, $P < 0.0001$. (f) Intracellular IFN-γ staining in gated CD3$^+$CD8β$^+$ T cells after stimulation with PMA and ionomycin for 6 h. Percent positive indicated where appropriate. Data in c–f are representative of four different experiments.

Gal-9 controls the functional activity of 4-1BB in T cells

As shown above, T cells are a major target of both positive and negative regulatory activities controlled by 4-1BB (Lee and Croft, 2009), and Gal-9 has been reported to be expressed by T cells either intracellularly or produced as a soluble molecule (Matsumoto et al., 1998). To determine whether the requirement for Gal-9 in the activity of anti–4-1BB was direct and intrinsic to the potential target cell of the antibody, we assessed expression and activity of 4-1BB in vitro in the absence of Gal-9. Anti-CD3/CD28–activated CD8 T cells had high levels of 4-1BB, but had little/no detectable surface expression of Gal-9 (Fig. 3 a). Whether this was caused by a lack of Gal-9 or because Gal-9 was masked from the detecting antibody used in flow was not clear; however, modifying the staining protocol in several ways, including fixing the cells before or after staining, did not alter the inability to detect surface Gal-9 (not depicted). Activated Gal-9$^{-/-}$ CD8 T cells were able to express 4-1BB on their surface, but at a slightly lower level compared with WT T cells, contrasting with another inducible TNFR molecule OX40 (Fig. 3 b). An agonistic antibody to 4-1BB (clone 3H3) was used for our functional studies. To show that this antibody effectively bound to 4-1BB on Gal-9$^{-/-}$ T cells, we in vitro–activated T cells from WT and Gal-9$^{-/-}$ mice and FACS-sorted these cells based on similar 4-1BB expression using a different anti–4-1BB (clone 17B5). Staining and flow cytometry of these cells with clone 3H3 revealed that this agonist antibody was capable of binding to 4-1BB on activated Gal-9$^{-/-}$ T cells similar to WT T cells (Fig. 3 c). To assess the function of 4-1BB where the expression level was not a factor, WT and Gal-9$^{-/-}$ CD8 T cells were preactivated and then sorted based on equivalent expression (Fig. 3 d). The T cells were restimulated with anti-CD3 in the presence of the agonist anti–4-1BB. WT and Gal-9$^{-/-}$ T cells responded equivalently when stimulated with anti-CD3 making low levels of IFN-γ. However, Gal-9$^{-/-}$ T cells were specifically hyporesponsive

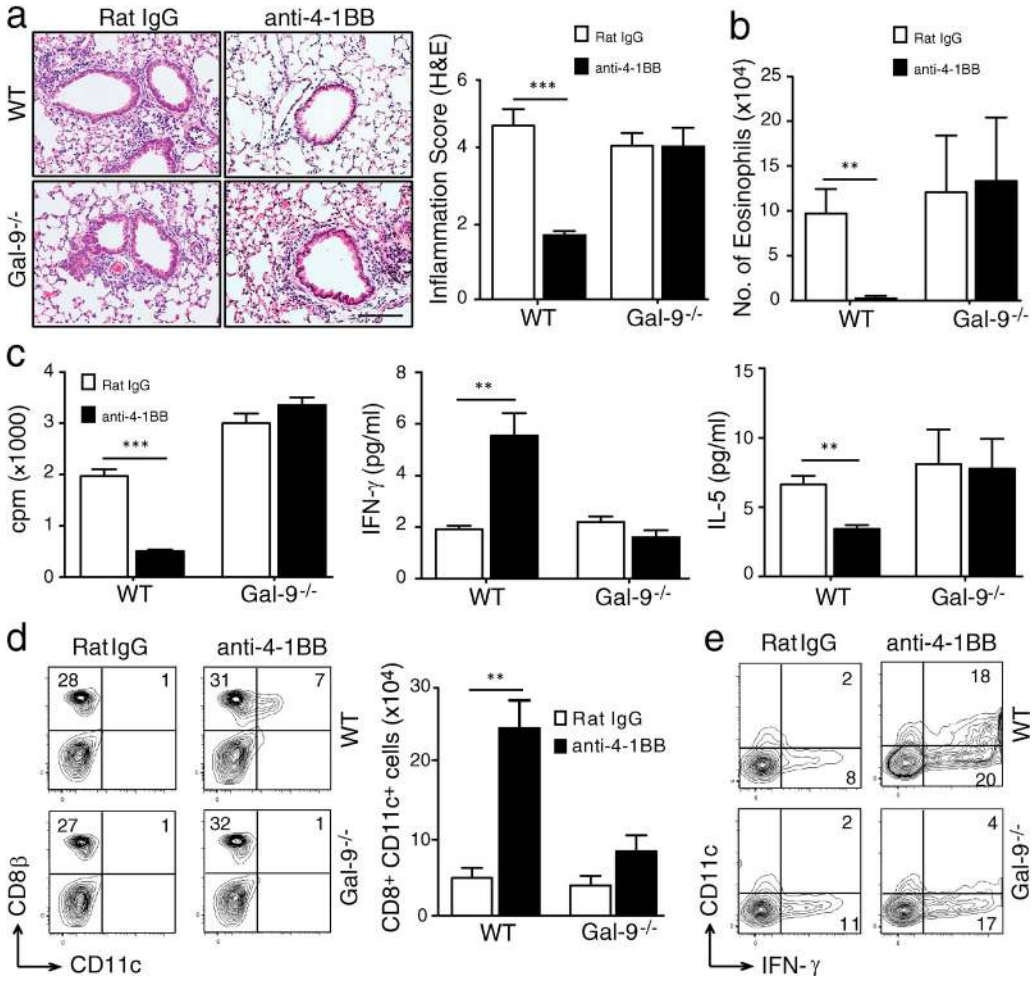

Figure 2. Gal-9 is required for suppression of allergic asthma by anti–4-1BB in vivo. WT and Gal-9$^{-/-}$ mice were immunized with OVA to induce lung inflammation and injected with rat IgG or agonist anti–4-1BB as described in Materials and methods, and mice were sacrificed on day 18. (a) Representative H&E staining of lung sections (left) and inflammation score (right) from four mice per group. Bar, 200 µm. (b) Quantification of eosinophil numbers in BAL. (c) [^{3}H]TdR thymidine incorporation (left) and IFN-γ (middle) and IL-5 production (right) in cultures of lung-draining LN cells stimulated in vitro with 200 µg/ml OVA for 72 h. (d) Proportion of gated CD3$^+$ cells in draining LNs expressing CD8β and CD11c (left) and total numbers (right). (e) Intracellular IFN-γ staining in gated CD3$^+$CD8β$^+$ T cells after stimulation with PMA and ionomycin for 6 h. Percent positive indicated where appropriate. All results are means ± SEM from four mice per group and are representative of three independent experiments. **, P < 0.01; ***, P < 0.001.

to anti–4-1BB and made significantly less cytokine (Fig. 3 d). To extend these results, 4-1BB–sorted CD8 T cells were stimulated with anti-CD3, and 4-1BB signaling was triggered by coculturing with transfected hybridoma cells that expressed high levels of 4-1BBL. This membrane version of 4-1BBL strongly co-stimulated IFN-γ production in WT T cells, as shown by blockade with an antibody to 4-1BBL. In contrast, Gal-9$^{-/-}$ T cells were much less responsive to the 4-1BBL$^+$ hybridoma cells, and any response they gave was not dependent on 4-1BB–4-1BBL interactions (Fig. 3 e). Similar results were seen when T cells were stimulated with recombinant 4-1BBL (Fig. 3 f). These data supported the hypothesis that either production of Gal-9 by the T cells was responsible for the enhanced cytokine secretion after triggering 4-1BB or, alternatively, that Gal-9 was required for 4-1BB to signal effectively when ligated.

Showing this was not restricted to CD8 T cells, we also obtained similar results with cytokine production by CD4 T cells and with regulation of the immunosuppressive enzyme retinal dehydrogenase (RALDH) in DCs, which controls the induction of Foxp3$^+$ regulatory CD4 T cells. Anti–4-1BB failed to induce IL-2 production in CD4 T cells deficient in Gal-9 sorted to express equivalent levels of 4-1BB (Fig. 3 g). Gal-9 was also not detectable on the membrane of activated CD4 T cells, but it was coexpressed on the surface of DC with 4-1BB (Fig. 3, g and h). Anti–4-1BB promoted RALDH activity in TLR2-ligand stimulated WT DCs, as shown previously (Lee et al., 2012). However, it was unable to up-regulate RALDH in Gal-9$^{-/-}$ DCs even though signaling through TLR2 induced normal low levels of RALDH activity, further showing specificity in the 4-1BB–Gal-9 axis (Fig. 3 i).

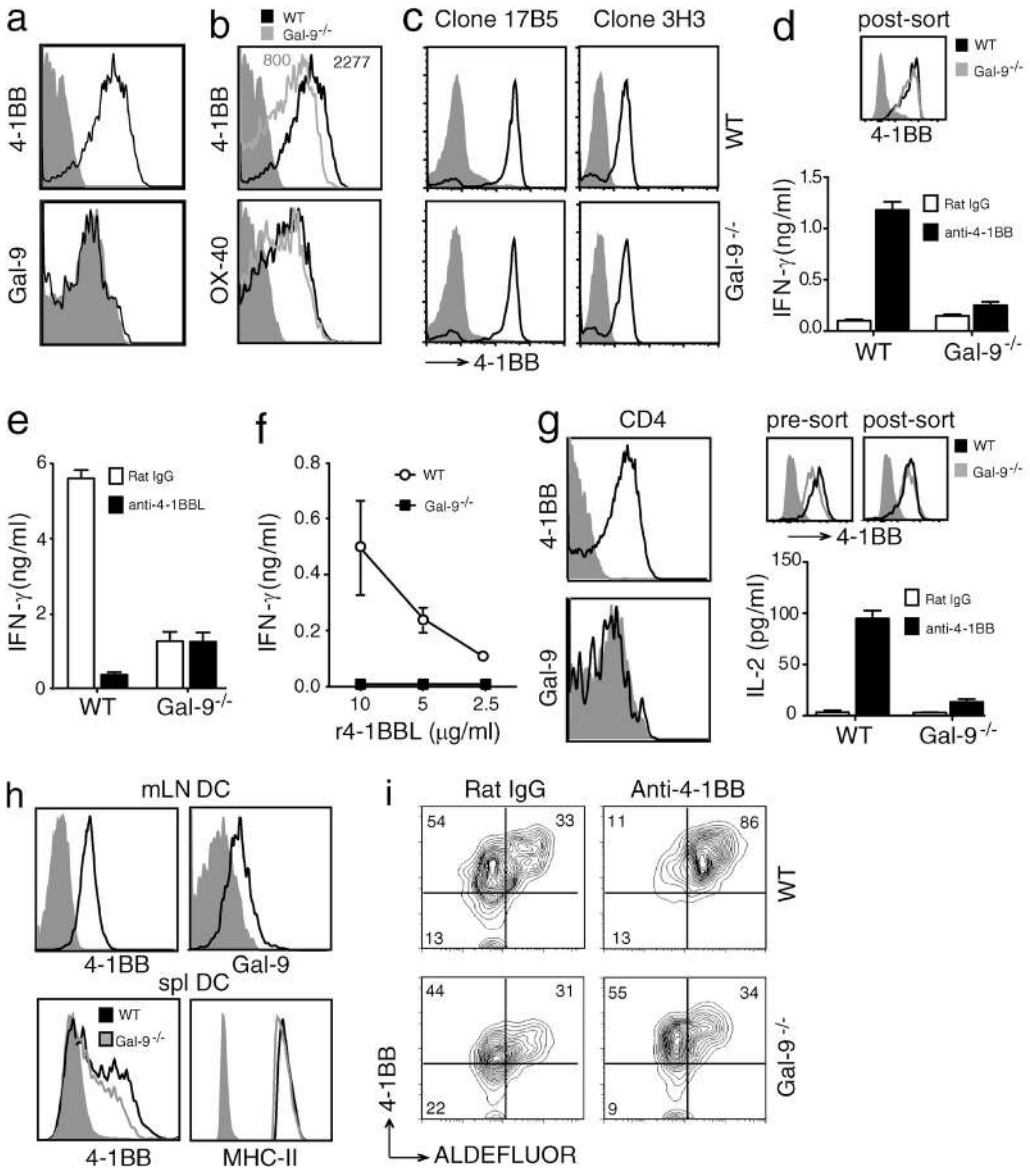

Figure 3. Defective 4–1BB activity in T cells and DCs from Gal-9$^{-/-}$ mice. (a) Surface expression of 4-1BB (top) and Gal-9 (bottom) in splenic CD8$^+$ T cells activated in vitro with anti-CD3 and anti-CD28 for 72 h. Shade, isotype control. (b) 4-1BB and OX40 surface expression on WT and Gal-9$^{-/-}$ CD8$^+$ T cells activated as in panel a. Mean fluorescent intensity indicated for 4-1BB. Shade, isotype control. (c) Binding of anti–4-1BB (clone 3H3) to activated CD8$^+$ T cells. Activated CD8$^+$ T cells as in panel a were sorted for identical expression of 4-1BB using biotin-anti–4-1BB (Syrian hamster IgG; clone 17B5) and streptavidin-APC. Cells were then stained with unlabeled anti–4-1BB (rat IgG; clone 3H3) and anti–rat IgG FITC to detect anti–4-1BB (clone 3H3) binding to cells. Shade, isotype controls. Data are representative of two different experiments. (d) IFN-γ production by preactivated CD8$^+$ T cells, from WT or Gal-9$^{-/-}$ mice, sorted for identical expression of 4-1BB (postsort FACS plot shown) and restimulated with plate-bound anti-CD3 in the presence of control rat IgG or anti–4-1BB for 24 h. Data are means ± SEM from triplicate cultures and representative of at least three different experiments. (e and f) CD8$^+$ T cells from WT or Gal-9$^{-/-}$ mice were activated as in panel a, sorted for identical expression of 4-1BB, and re-cultured for another 24 h to assay IFN-γ production in response to irradiated 4-1BBL$^+$ hybridoma cells (e) or varying concentrations of anti-polyhistidine cross-linked r4-1BBL (f). Neutralizing anti–4-1BBL or rat IgG was added to cultures in e. Data are means ± SEM from triplicate cultures and representative of two different experiments. (g, left) Surface expression of 4-1BB (top) and Gal-9 (bottom) in splenic CD4 T cells activated in vitro with anti-CD3 and anti-CD28 for 72 h. Shade, isotype control. (right) IL-2 production by preactivated CD4$^+$ T cells, from WT or Gal-9$^{-/-}$ mice, sorted for identical expression of 4-1BB (pre- and postsort FACS plot shown), and restimulated with plate-bound anti-CD3 in the presence of control rat IgG or anti–4-1BB for 24 h. Data are means ± SEM from triplicate cultures and representative of three different experiments. (h) Surface expression of 4-1BB and Gal-9 (top) and 4-1BB and MHC II (bottom) on ex vivo WT mesenteric LN DCs and splenic DCs from WT and Gal-9$^{-/-}$ mice cultured with GM-CSF, respectively. Shade, isotype control. (i) ALDEFLUOR staining in preactivated spleen DCs from WT and Gal-9$^{-/-}$ mice, sorted for identical expression of 4-1BB, and recultured for 24 h in the presence of zymosan with control rat IgG (left) or agonist anti–4-1BB (right). Numbers indicate percentage of cells in each quadrant. Data are representative of three different experiments.

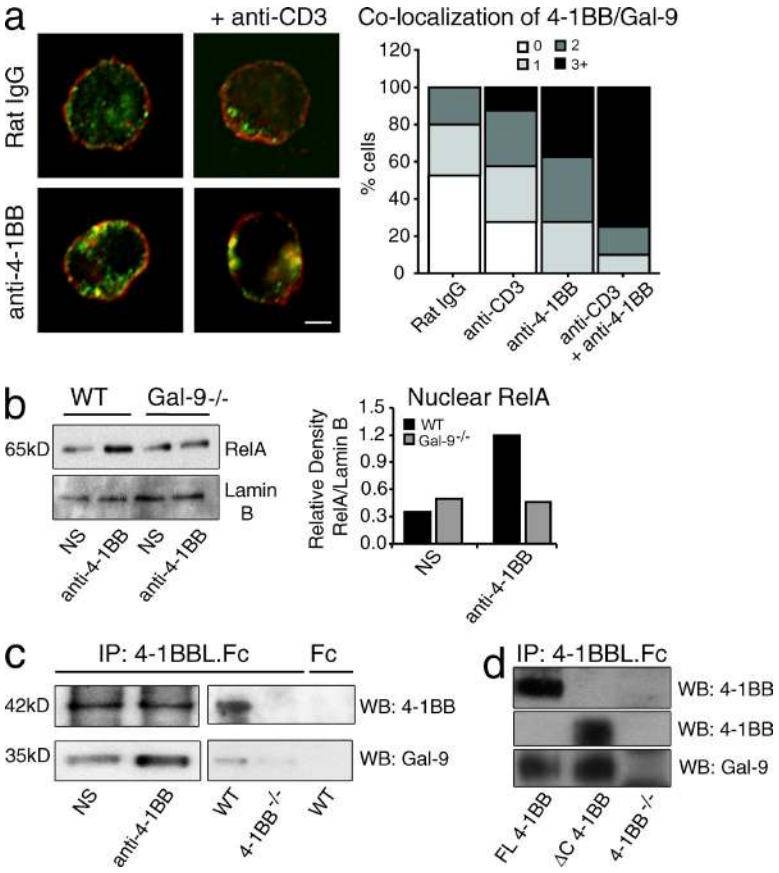

Figure 4. Gal-9 colocalizes with 4-1BB. (a) Confocal analysis of 4-1BB (red) and Gal-9 (green) in preactivated WT CD4+ T cells cultured with agonist anti–4-1BB or rat Ig in the presence or absence of anti-CD3 for 15 min. Percent colocalization of 4-1BB and Gal-9 from confocal images is shown on the right. Cells analyzed (40 cells per group) showing zero, one, two, or more than three colocalization spots per cell in each group are shown as a percentage of total cells. Data are representative of two different experiments. Bar, 1 µm. (b) Western blot of translocated nuclear RelA in preactivated CD4+ T cells from WT and Gal-9$^{-/-}$ mice cultured with agonist anti–4-1BB or without stimulation (NS) for 30 min. Lamin B was used as a nuclear loading control. Relative density of RelA to Lamin B quantified by ImageJ software (National Institutes of Health) is shown on the right. Data are representative of at least three different experiments. (c, left) 4-1BB immunoprecipitated (IP) with 4-1BBL.Fc from preactivated WT CD4+ T cells that were cultured with agonist anti–4-1BB or without stimulation (NS) for 30 min. (right) 4-1BB was immunoprecipitated with 4-1BBL.Fc or Fc control from preactivated WT or 4-1BB$^{-/-}$ CD4+ T cells. Western blots (WB) were performed to detect 4-1BB and Gal-9. Data are representative of two different experiments. (d) 4-1BB was immunoprecipitated with 4-1BBL.Fc from 4-1BB$^{-/-}$, full-length (FL), or ΔC 4-1BB–transduced T hybridoma cells. Western blots were performed to detect 4-1BB and Gal-9 (molecular masses are the same as for c). Data are representative of two different experiments.

Gal-9 colocalizes with 4-1BB and is a binding partner for 4-1BB

Although Gal-9 was not detectable on the surface of activated T cells, confocal imaging showed that Gal-9 was expressed intracellularly (Fig. 4 a). After ligating 4-1BB, we did not detect Gal-9 in the supernatant of the T cells (not depicted); however, cross-linking 4-1BB alone, or CD3 with 4-1BB, promoted a significant fraction of Gal-9 to colocalize at the membrane with a fraction of 4-1BB (Fig. 4 a), implying that Gal-9 might help 4-1BB to signal. Correlating with this, we assessed activation of a primary signaling pathway of 4-1BB in T cells, namely NF-κB, and found that ligation of 4-1BB could not effectively augment accumulation of nuclear RelA in Gal-9$^{-/-}$ T cells (Fig. 4 b). In line with this, precipitation of 4-1BB from activated T cells with 4-1BBL.Fc revealed low levels of Gal-9 before ligation, but the amount coprecipitated was strongly increased when 4-1BB was cross-linked with antibody (Fig. 4 c, left blot). 4-1BBL.Fc did not precipitate Gal-9 from 4-1BB$^{-/-}$ cells, suggesting this result reflected co-association of 4-1BB with Gal-9 (Fig. 4 c, right blot). To further investigate this, we generated a hybridoma from activated 4-1BB$^{-/-}$ T cells and transduced this with full-length 4-1BB or a mutant 4-1BB lacking the cytoplasmic region (ΔC). Gal-9 was coprecipitated with either full-length or ΔC4-1BB, suggesting that Gal-9 might directly bind the extracellular region of 4-1BB (Fig. 4 d). These data suggested that 4-1BB could associate directly or indirectly with endogenously produced Gal-9 on the membrane of cells. As the Galectin family interacts at least in part with oligosaccharide side chains of glycoproteins (Rabinovich et al., 2007; Rabinovich and Toscano, 2009), the colocalization of Gal-9 induced by cross-linking 4-1BB and CD3 on T cells may be related to increasing the local glycan concentration that can readily bind to Gal-9. Another possibility is that ligation of 4-1BB might alter cellular glycosylation and change the type of N-glycans displayed to those with higher avidity for Gal-9.

To extend this to another 4-1BB–expressing immune cell, we focused on NK cells. IL-2–activated splenic NK cells from Gal-9$^{-/-}$ mice exhibited less membrane 4-1BB but not other markers such as NK1.1 (Fig. 5 a), but sorting activated WT and Gal-9$^{-/-}$ NK cells based on identical levels of 4-1BB still revealed an inability of anti–4-1BB to effectively induce IFN-γ production when Gal-9 was absent (Fig. 5 b). As a control, anti-NK1.1 was able to induce IFN-γ in both WT and Gal-9$^{-/-}$ NK cells. Similar results were seen when NK cells were stimulated with recombinant 4-1BBL (Fig. 5 c). Unlike T cells, NK cells expressed membrane Gal-9 by flow cytometry regardless of ligation of 4-1BB (Fig. 5 d). Confocal imaging confirmed strong surface expression and colocalization of a proportion of both molecules. Additionally, cross-linking 4-1BB resulted in greater clustering of 4-1BB with Gal-9 (Fig. 5 e). Lastly, immunoprecipitation of 4-1BB from NK cells also pulled down Gal-9 (Fig. 5 f).

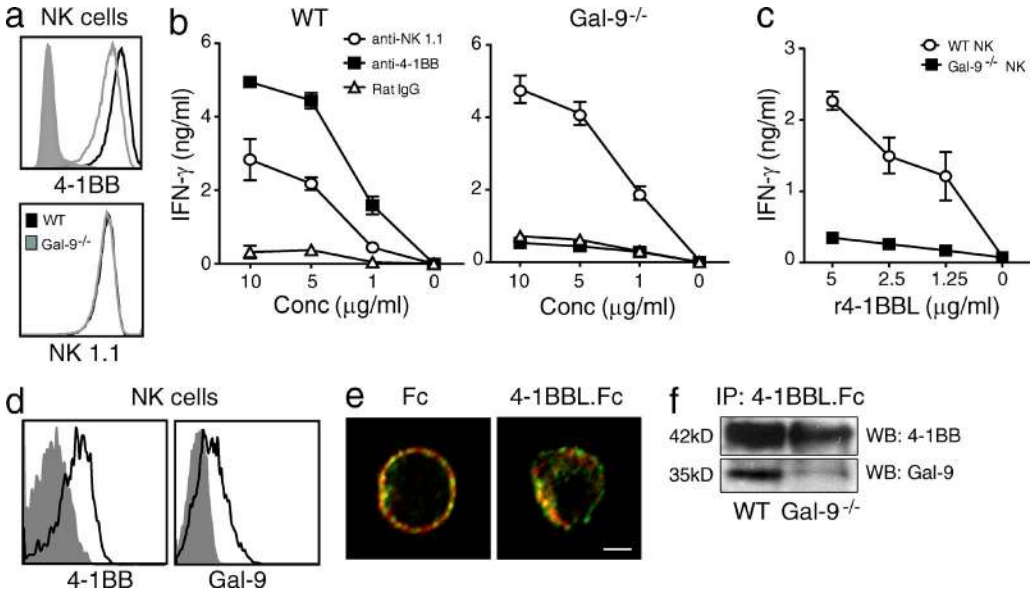

Figure 5. Defective 4-1BB activity in Gal-9–deficient NK cells. (a) Expression of 4-1BB (top) and NK1.1 (bottom) on IL-2–activated splenic NK cells from WT and Gal-9$^{-/-}$ mice. Shaded histogram, isotype control for 4-1BB. (b and c) NK cells were preactivated as in panel a and then sorted for identical expression of 4-1BB. Cells were cultured for 2 d in the presence of varying concentrations of agonist anti–4-1BB or anti-NK1.1, or control IgG (b) or antihistidine cross-linked r4-1BBL (c), and secretion of IFN-γ was assayed. Data are means ± SEM from triplicate cultures and representative of three different experiments. (d) Flow analysis of surface expression of 4-1BB and Gal-9 on ex vivo NK cells from spleen. Shaded histograms, isotype control. (e) Confocal detection of 4-1BB (red) and Gal-9 (green) on IL-2–activated WT NK cells cultured with 5 μg/ml 4-1BBL.Fc or 5 μg/ml of control human Fc for 15 min. Data are representative of two different experiments. Bar, 1 μm. (f) 4-1BB was immunoprecipitated (IP) with 4-1BBL.Fc from IL-2–activated WT and Gal-9$^{-/-}$ NK cells, followed by detection of 4-1BB and Gal-9 by Western blotting (WB). Data are representative of at least three different experiments.

Together, these data suggested that Gal-9 inducibly or constitutively associates with 4-1BB on the membrane of T cells, DCs, and NK cells to allow 4-1BB to be functional. To test whether Gal-9 directly binds to 4-1BB, we used a binding assay in which recombinant mouse Gal-9 or 4-1BBL was coated onto a plate, and a fusion protein containing the extracellular region of mouse 4-1BB (4-1BB.Fc) was used to screen for binding activity. Another member of the Galectin family (Gal-1) and an irrelevant Fc fusion protein (BTLA.Fc) were used as controls. 4-1BB showed binding activity for both Gal-9 and 4-1BBL, but not for Gal-1 (Fig. 6 a). We further tested binding using a fluorescence assay, in which mouse 4-1BB.Fc or control Fc was coated onto protein G beads and binding of mouse Gal-9 or 4-1BBL was visualized by flow cytometry. Again, both Gal-9 and 4-1BBL showed specific binding activity to 4-1BB.Fc (Fig. 6 b). Gal-3 also did not bind to 4-1BB as a further control.

To determine whether this interaction is conserved across species, we performed coimmunoprecipitation experiments with human or mouse Gal-9 and Fc fusion proteins of the extracellular regions of human or mouse 4-1BB. Both human and mouse 4-1BB.Fc were able to precipitate human and mouse Gal-9 (Fig. 6 c). Human 4-1BBL precipitated with either human or mouse 4-1BB.Fc, whereas mouse 4-1BBL precipitated only with mouse 4-1BB.Fc, as previously shown (Bossen et al., 2006). Gal-4 was used as a further control and was not precipitated by either human or mouse 4-1BB.Fc (Fig. 6 c). We then assessed the dynamics of binding of mouse and human 4-1BB with mouse and human Gal-9 using SPR. The respective interactions were found to exhibit equilibrium binding constants (K_d) of ∼11 and ∼85 nM, with the enhanced overall binding of mouse Gal-9 with mouse 4-1BB largely explained by a slower off rate (Fig. 6, d and e).

Our functional and immunoprecipitation experiments suggested that the binding site for Gal-9 did not overlap with the binding sites for anti–4-1BB or 4-1BBL. To formally show this, protein G beads were coated with mouse 4-1BB.Fc and preincubated with saturating concentrations of either mouse 4-1BBL or Gal-9 before incubation with Gal-9 or 4-1BBL, respectively (Fig. 6 f). In both cases, we were able to detect the alternate molecule on the same beads. We further found that the agonistic antibody of mouse 4-1BB (clone 3H3) used in our in vivo experiments and another agonist (clone 1D8; Shuford et al., 1997) also did not block binding of Gal-9 to 4-1BB (Fig. 6 f). In summary, Gal-9 can interact with the extracellular region of 4-1BB in a manner that does not compete with the known ligand of 4-1BB or stimulatory antibodies that promote 4-1BB immunomodulatory activity, and the interaction with Gal-9 is conserved between the mouse and human.

Both domains of Gal-9 bind to CRD4 of 4-1BB in a carbohydrate-dependent manner

To formulate a mechanistic understanding of this interplay and why Gal-9 was required for the activity of anti–4-1BB

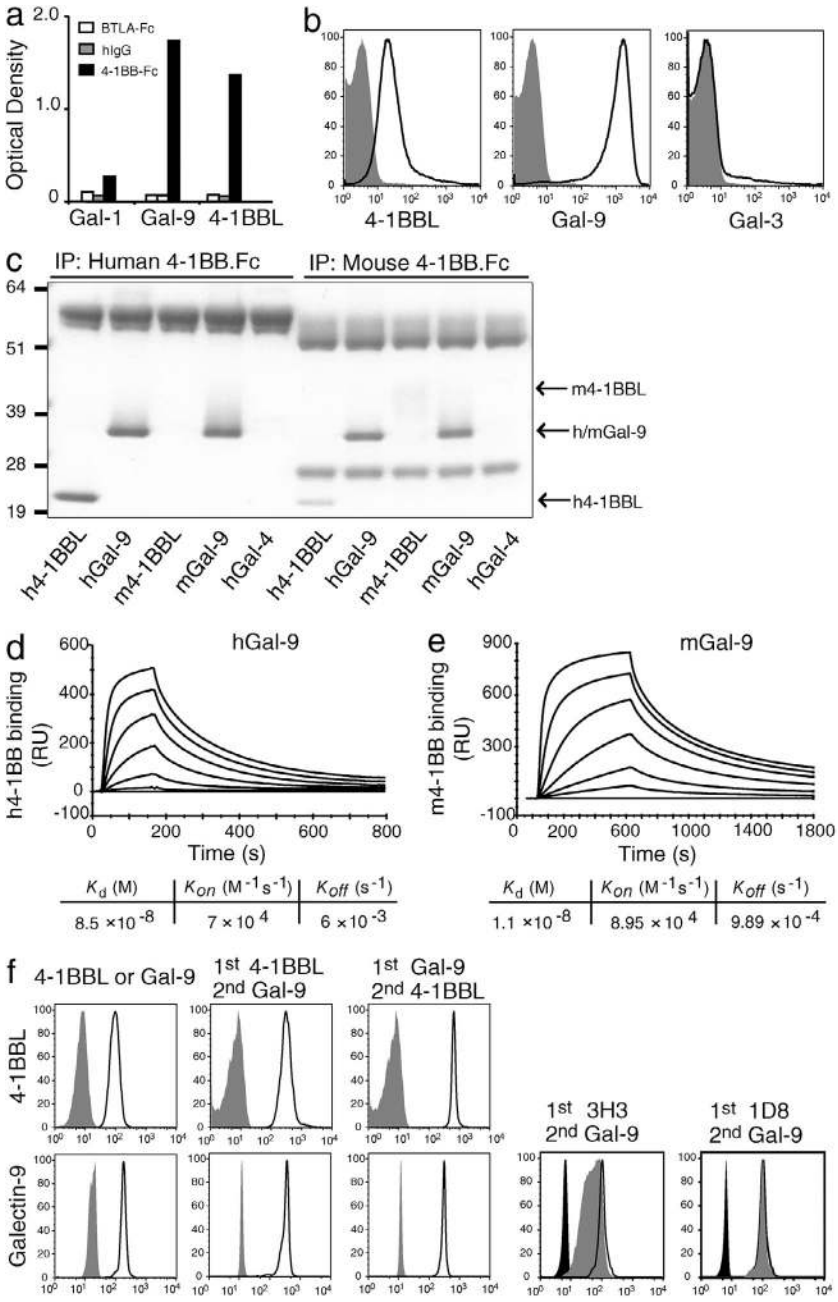

	K_d (M)	K_{on} ($M^{-1}s^{-1}$)	K_{off} (s^{-1})
d	8.5×10^{-8}	7×10^{4}	6×10^{-3}
e	1.1×10^{-8}	8.95×10^{4}	9.89×10^{-4}

Figure 6. Gal-9 binds to 4-1BB. (a) Binding of m4-1BB.Fc or mBTLA.Fc or control hIgG to plate-bound recombinant mGal-1, mGal-9, or m4-1BBL, as measured by optical density. (b) Flow cytometry detection of binding of recombinant m4-1BBL, mGal-9, or mGal-3 to saturating amounts of m4-1BB.Fc coated on protein G beads. Shaded histograms, binding to control hIgG (Fc fragment)–coated beads. (c) SDS-PAGE of coimmunoprecipitation of h/m4-1BBL, h/mGal-9, or h/mGal-4 with h4-1BB.Fc (left) or m4-1BB.Fc (right). The observed molecular masses (kilodaltons) were h/m4-1BB.Fc, 55–58; h4-1BBL, 20; m4-1BBL, 41–44; m/hGal-9, 36; and m/hGal-4, 36. Data in a–c are representative of at least three different experiments each. (d and e) Binding response of increasing concentrations (0.004–0.312 µM) of hGal-9 (d) or mGal-9 (e) to immobilized h4-1BB.Fc (d) or m4-1BB.Fc (e), as measured by SPR. Values represent the mean of three independent measurements. The response shown is reference-subtracted (unrelated Fc protein). (f) Flow analysis of competition between m4-1BBL/anti–4-1BB antibodies and mGal-9 for binding to m4-1BB.Fc. m4-1BB.Fc–coated protein G beads were incubated either with m4-1BBL (top left) or mGal-9 (bottom left) alone. For competition between m4-1BBL and mGal-9, m4-1BB.Fc–coated beads were first incubated with m4-1BBL (second left) or mGal-9 (middle). The beads were washed and incubated further with mGal-9 (second left) or m4-1BBL (middle). Binding of m4-1BBL (top) or mGal-9 (bottom) was detected using different fluorescent-labeled antibodies and analyzed by flow. Shaded histogram, binding of respective detection antibody isotype. For competition between anti–4-1BB antibodies and mGal-9, m4-1BB.Fc–coated beads were first incubated with agonistic 4-1BB antibodies, clone 3H3 (second right) or 1D8 (right). The beads were washed and further incubated with mGal-9. Open black histograms, mGal-9 binding without anti-4-1BB antibodies. Gray-shaded histograms, mGal-9 binding after anti-4-1BB antibodies. Black-shaded, beads with no mGal-9. Data are representative of two different experiments.

and 4-1BBL, we loosely mapped the binding sites of Gal-9 and 4-1BB. The extracellular portion of 4-1BB contains four CRDs (Kwon and Weissman, 1989; Kwon et al., 1994), where CRD1 is farthest and CRD4 is closest to the cell membrane. We then constructed soluble variants of the extracellular region of human and mouse 4-1BB as Fc fusion proteins containing alternate CRDs. It is not known where human 4-1BBL binds to human 4-1BB, but modeling based on other TNFR family complexes suggested somewhere within the first three CRDs (Loo et al., 1997). Supporting this, human 4-1BBL was immunoprecipitated with a human 4-1BB mutant containing CRD1, -2, and -3, but significantly not with a mutant containing only CRD4 (Fig. 7 a). In contrast, human Gal-9 and mouse Gal-9 were precipitated with the CRD4 construct, but not with the CRD1–3 construct. To further test this in a more sensitive assay, we performed SPR analysis of both human (Fig. 7 b) and mouse (Fig. 7 c) 4-1BB mutants with human and mouse Gal-9, respectively. Strong binding to CRD4 was detected in both cases. Human Gal-9 showed no specific binding activity with human 4-1BB CRD1–3. Mouse Gal-9 showed moderate binding activity with mutants of mouse 4-1BB containing CRD1 and -2 or CRD2 and -3. However, this was considerably less than that observed with mutants containing CRD3 and -4 or CRD4 alone. A previous study suggested that mouse 4-1BBL binds primarily in CRD1 and -2 (Loo et al., 1997), and we confirmed this in

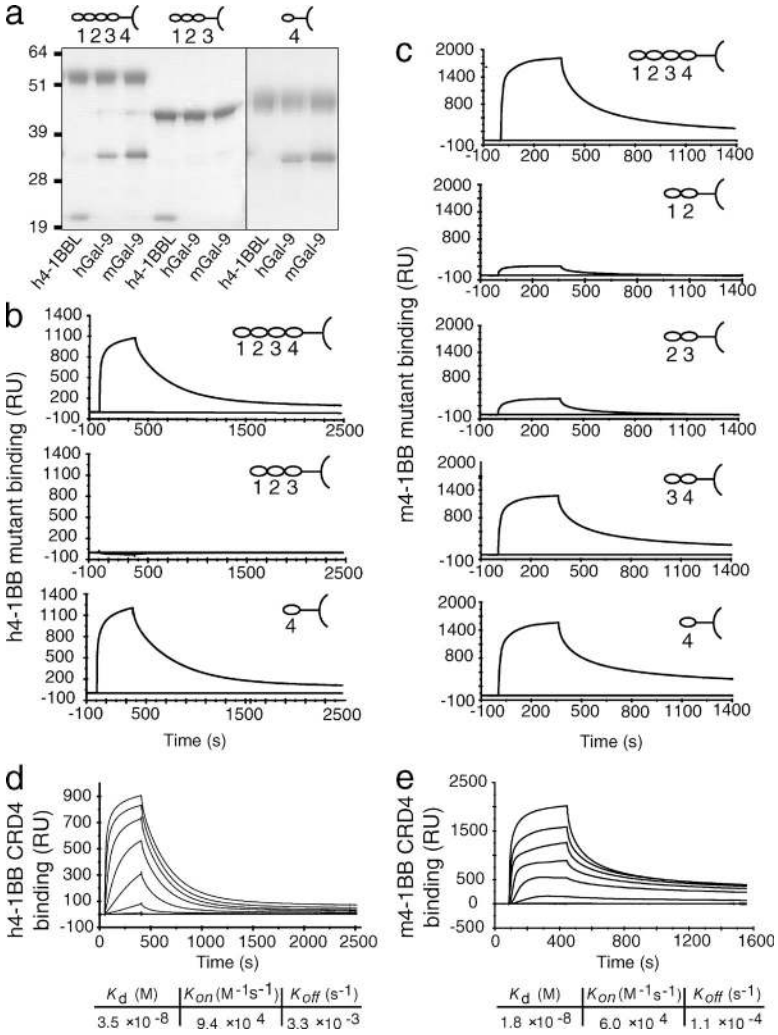

Figure 7. Gal-9 binds to CRD4 of 4-1BB. (a) Coimmunoprecipitation of recombinant h4-1BBL or h/mGal-9 with full-length (CRD1–4), CRD1–3, or CRD4 h4-1BB.Fc constructs. The observed molecular masses (kilodaltons) were FL h4-1BB.Fc, 55; CRD1–3 h4-1BB.Fc, 44; CRD4 h4-1BB.Fc, 47–49; h4-1BBL, 20; and m/hGal-9, 36. Data are representative of at least three different experiments. (b and c) Binding response of a single concentration (2.5 µM) of hGal-9 or mGal-9 with the indicated immobilized CRD mutants of h4-1BB.Fc (b) or m4-1BB.Fc (c), respectively, as measured by SPR. The response shown is reference-subtracted (human Fc). Data are representative of three different experiments. (d and e) Binding response of increasing concentrations (0.004–0.312 µM) of hGal-9 (d) or mGal-9 (e) to immobilized CRD4 mutants of h4-1BB.Fc (d) or m4-1BB.Fc (e), as measured by SPR. Values represent the mean of two independent measurements.

detecting strong binding to the CRD1–2 and CRD2–3 constructs, but not constructs containing only CRD3 and -4 or CRD4 alone (not depicted). We then determined the K_d of human 4-1BB CRD4 binding to human Gal-9 to be ∼35 nM and mouse 4-1BB CRD4 with mouse Gal-9 to be ∼18 nM (Fig. 7, d and e). These values were sufficiently close to those with full-length 4-1BB (Fig. 6, d and e) to further suggest that human and mouse Gal-9 primarily bind to CRD4 of human and mouse 4-1BB, respectively.

It is generally acknowledged that TNFR family molecules are not functional as monomers, in line with the majority of their ligands being natural trimers that have the potential to bind and recruit several monomers. As Gal-9 bound CRD4 and did not compete for the binding sites of 4-1BBL or agonist antibodies, this suggested that Gal-9 might function by promoting the association of two or more monomers of 4-1BB such that they cluster together efficiently. Gal-9 is a tandem-repeat molecule possessing two domains, termed N- and C-, joined by a flexible linker. These domains have only 39% amino acid sequence similarity (Türeci et al., 1997), but both have been found to possess high affinity for certain branched bi-, tri-, and tetra-antennary N-linked glycans with *N*-acetyllactosamine motifs (Hirabayashi et al., 2002; Sato et al., 2002). This suggests that one molecule of Gal-9 may have the potential to bind two molecules of 4-1BB. Alternatively, the C-terminal domain of Gal-9 was found to self-associate via the surface opposite to its carbohydrate-binding sites (Nonaka et al., 2013), and the N-terminal domain was also suggested to self-dimerize (Nagae et al., 2006), which would allow two or more molecules of 4-1BB to be linked by two or more molecules of Gal-9. To determine whether one or both domains could bind 4-1BB, we tested constructs containing the N- or the C-domain in isolation. Immunoprecipitation experiments revealed that both domains of Gal-9 could bind full-length 4-1BB as well as CRD4 of 4-1BB (Fig. 8 a).

Both human and mouse 4-1BB have predicted N-linked glycosylation sites. Mouse 4-1BB has a possible glycosylation site in each of its four CRDs. However, there are two predicted sites in CRD4 of human 4-1BB, one of which is common to CRD4 of mouse 4-1BB, in line with Gal-9 binding to CRD4 in a carbohydrate-dependent manner. We

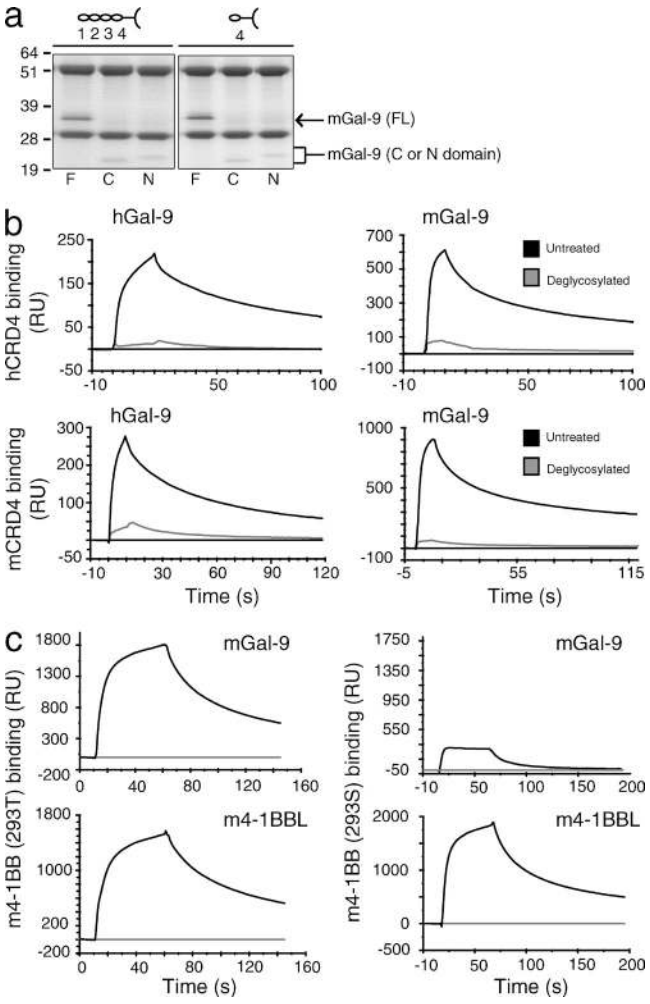

Figure 8. Gal-9 binding to 4-1BB is carbohydrate dependent. (a) Coimmunoprecipitation of full length (F), C-terminal (C), or N-terminal (N) mGal-9 mutants with full-length (CRD1-4) or CRD4 m4-1BB.Fc. The observed molecular masses (kilodaltons) were FL m4-1BB.Fc, 55; CRD4 m4-1BB.Fc, 51; FL mGal-9, 36; C-terminal mGal-9, 21; and N-terminal mGal-9, 23. Data are representative of two different experiments. (b) Binding response of a single concentration (2.5 µM) of human (right) or mouse (left) Gal-9 to immobilized CRD4 of human (top) or mouse (bottom) 4-1BB.Fc, as measured by SPR. Black and gray lines indicate untreated or deglycosylated (PNGase F/Endo H treated) CRD4 4-1BB.Fc, respectively. The response shown is reference-subtracted (human Fc). Data are representative of two different experiments. (c) Binding response of 2.5 µM mouse Gal-9 (top) or 5 µM mouse 4-1BBL (bottom) to immobilized mouse 4-1BB.Fc produced in HEK 293T cells (left) or HEK 293S cells (right), as measured by SPR. The response shown is reference-subtracted (human Fc - gray line). Data are representative of three different experiments.

therefore deglycosylated human and mouse CRD4 mutant 4-1BB.Fc constructs by treating with PNGase F/Endo H enzymes to remove N-linked sugars. Based on SPR analysis, this resulted in greatly reduced binding activity of both human and mouse Gal-9 (Fig. 8 b). We further produced 4-1BB.Fc in 293S cells that lack *N*-acetylglucosaminyltransferase I (GnTI) and thus cannot produce complex N-glycans. We observed a similar result with a substantial reduction in the ability of 4-1BB to bind to Gal-9 but no effect on the ability to bind to 4-1BBL (Fig. 8 c). Thus, Gal-9 has the potential to cross-link 4-1BB monomers in a carbohydrate-dependent manner via the fourth, most membrane-proximal, CRD. These data collectively suggest that Gal-9 is an essential co-receptor that allows 4-1BB monomers to cluster when ligated by conventional agonist antibodies or its TNF ligand, and Gal-9 permits 4-1BB molecules to aggregate in a manner that is crucial for mediating the functional and therapeutic activity of agonist anti–4-1BB.

DISCUSSION

In summary, we describe a new molecule that facilitates the therapeutic activity of agonist antibodies against a TNFR superfamily member. These results also highlight a new paradigm in the TNFR family for structural organization of monomers into a signaling unit and suggest that the interaction of 4-1BB with Gal-9 may be a future target for both positively and negatively manipulating the immune response.

One activity of Gal-9 is to stabilize the surface expression of 4-1BB, as shown by reduced levels on T cells, DCs, and NK cells in Gal-9–deficient mice. Together with our confocal and flow data detecting Gal-9 in these cells, this implies that the source of Gal-9 for binding to 4-1BB is intrinsic. Nevertheless, we cannot rule out the possibility that in vivo Gal-9 might be available extrinsically as it can be produced as a soluble molecule. Interestingly, Gal-9 was reported to be colocalized with glucose transporter 2 on pancreatic β cells, and indirect data suggested it might influence the rate of glucose transporter 2 endocytosis (Ohtsubo et al., 2005). Exogenously added Gal-9 was also suggested to complex directly or indirectly with protein disulfide isomerase in a T cell line, and this increased the ability to detect the molecule on the surface of these cells (Bi et al., 2011). Thus, Gal-9 may participate in regulating the cycling of 4-1BB and other proteins from internal compartments to the surface of cells.

Regardless of membrane levels of 4-1BB in T cells, DCs, or NK cells, compensating for the variation in expression in the absence of Gal-9 did not restore cellular activity when 4-1BB was ligated. Our data then lead to several models for how Gal-9 may control the function of 4-1BB (depicted in Fig. S1, a–c). The first model is based on the crystal structure of 4-1BBL and the notion that the spatial distribution of TNFR family monomers may impact how effectively a TNF family ligand can promote functional activity (Fig. S1 a). Whereas many TNFR ligands such as TNF and LTα are trimers with a bell shape (Bodmer et al., 2002), a group of molecules including 4-1BBL, GITRL, and OX40L have been visualized to diverge from this structure and display an open trimeric configuration reminiscent of a blooming flower (Compaan and Hymowitz, 2006; Chattopadhyay et al., 2007; Zhou et al., 2008; Won et al., 2010). From the crystal structures of the complexes of three OX40 monomers with OX40L and three GITR monomers with GITRL, it has

then been estimated that the monomers of OX40 and GITR when bound to their ligands may be separated by a greater distance (45–70 Å) than monomers of TNFR family molecules when bound to bell-shaped TNF ligands (20–35 Å; Chattopadhyay et al., 2009). As the structure of 4-1BBL revealed it to be an even more open and extended propeller-like structure (Won et al., 2010), this implies that 4-1BB monomers might be separated by a large distance in the cell membrane when engaged by 4-1BBL (Fig. S1 a, left). This might not result in productive signaling. Through its ability to engage 4-1BB monomers through CRD4, Gal-9 may then spatially reorientate the membrane-proximal and intracellular domains into a closer configuration that is more conducive for productive signaling (Fig. S1 a, right).

This is an attractive model, but it may be too simplistic. Recombinant trimeric 4-1BBL in soluble form cannot induce functional activity in T cells unless it is cross-linked artificially (Rabu et al., 2005). This implies that even in the presence of Gal-9, recruiting three 4-1BB monomers may be unlikely to result in a cellular response. Therefore, another model, not mutually exclusive from the first, is that Gal-9 bridges aggregates of monomers of 4-1BB, which could include bringing dimers or trimers into close proximity on the cell membrane (Fig. S1 b). This might occur through bridging brought about by a single molecule of Gal-9, based on the data showing that both the N- and C-terminal domains possess the ability to bind 4-1BB. Alternatively, it could occur through dimers or higher-order multimers of Gal-9 that result through interdomain self-association (Nagae et al., 2006; Nonaka et al., 2013) or linker self-association, which has also been suggested for certain Galectins (Earl et al., 2011). The defective activity of the agonist antibody to 4-1BB in Gal-9–deficient cells further shows that Gal-9 plays a role in aggregation or clustering of sets of 4-1BB monomers. Theoretically, this antibody will engage only two monomers of 4-1BB. However, based on the inactivity of trimeric soluble 4-1BBL when not cross-linked, it would then be predicted that agonist antibodies that only bring two molecules of 4-1BB together should not be stimulatory. As this is not the case in Gal-9–expressing cells, this also supports a model in which Gal-9 allows multimerization of 4-1BB when two molecules of 4-1BB are engaged by an antibody (Fig. S1 c).

This conclusion draws parallels with the recent work showing that agonist antibodies designed to stimulate the TNFR family members TRAILR, CD40, and GITR depend on co-engagement with either stimulatory or inhibitory Fcγ receptors for robust activity (Nagae et al., 2006; Wilson et al., 2011). One study found that stimulatory Fcγ receptors were not required for the activity of anti–4-1BB (Schabowsky et al., 2009), and therefore, Gal-9–mediated clustering of 4-1BB may circumvent any requirement for binding of an antibody to Fc receptors (Fig. S1 c). Receptor oligomerization by galectins has been previously described for Gal-1 (Pace et al., 1999; Fulcher et al., 2009; Grigorian et al., 2009) but not greatly appreciated for Gal-9 nor in the TNFR family, or in the context of controlling the therapeutic activity of antibodies. The results here are additionally of great interest when considering the activity of other TNFR superfamily members. Although it is generally believed that the basic signaling unit in the TNFR family is a trimer, previous data with TNFR1, TNFR2, Fas, CD40, and the TRAIL receptors described a region in CRD1 of these molecules, termed a preligand assembly domain (PLAD), which has been hypothesized to control their function. This region allows self-association, enabling two monomers to aggregate in a ligand-independent manner (Chan et al., 2000; Siegel et al., 2000), leading to the proposal that the PLAD then facilitates aggregation of dimers of these aforementioned TNFR family molecules into higher-order lattice-like structures when engaged by their ligands (Chan, 2007). 4-1BB does not to our knowledge possess a PLAD, but instead our data suggest that Gal-9 performs a similar function, albeit at the opposite end of the molecule, to allow higher-order aggregates to form. Whether this property of Gal-9 to organize 4-1BB as a signaling molecule is specific for only 4-1BB in the TNFR superfamily is of obvious interest for future studies, as is the question of whether other Galectin family molecules may bind and cluster different TNFR family members. It was suggested some time ago that there was greater sequence conservation across species in CRDs 1 and 4 versus 2 and 3 in TNFR molecules (Naismith and Sprang, 1998), which could imply that monomer aggregation via PLAD or Galectin binding may be more common than previously appreciated. Gal-9 was recently immunoprecipitated with CD40 from activated T cells, although no data were presented to demonstrate direct binding between the molecules (Vaitaitis and Wagner, 2012). Nonetheless, this raises the likelihood that interactions between TNFR family molecules and Galectins, or some other type of coreceptor, are not confined to 4-1BB.

Our results also lead to further questions regarding how Gal-9 controls functional activity within the immune system. Gal-9 has been reported to bind Tim-3 and CD44 (Zhu et al., 2005; Katoh et al., 2007). Soluble recombinant Gal-9 has been injected into numerous mouse models of inflammatory disease, including EAE, arthritis, and diabetes models, and generally found to suppress disease activity (Zhu et al., 2005; Seki et al., 2007, 2008; Arikawa et al., 2009; Chou et al., 2009), leading to the notion that Gal-9 may be a future therapeutic for inhibiting autoimmune disease (Wiersma et al., 2013). It has generally been assumed that the action of Gal-9 in these scenarios is mediated through binding Tim-3, as Tim-3 is an intrinsically suppressive molecule. However, in many cases this has not been proven and additional binding partners may play a role. Moreover, several studies have shown activities of soluble Gal-9 that were Tim-3 independent (Su et al., 2011; Oomizu et al., 2012; Golden-Mason et al., 2013). Our results then raise the intriguing possibility that some of the activities of recombinant Gal-9 may be mediated in part through binding 4-1BB. Further studies in this area will be important to assess whether soluble Gal-9 does lead to any functional response involving signaling through 4-1BB. It will also be important to define all of the binding partners for Gal-9 and

whether 4-1BB complexes through bridging to Gal-9 with other glycoproteins such as Tim-3 to form new and novel signaling units.

In conclusion, Gal-9 is a novel 4-1BB–associating protein and a key regulator of the ability of anti–4-1BB to exert immunotherapeutic activity. Conserved binding between mouse and human proteins suggests this will be an important interaction in human disease. Given the potential impact of targeting 4-1BB and Gal-9 clinically, a greater understanding of this interaction may be critical for manipulating many immune function–related diseases such as cancer, infectious disease, and autoimmune disease.

MATERIALS AND METHODS

Mice. 8–10-wk-old C57BL/6 (WT) mice were purchased from the Jackson Laboratory. *Gal-9*$^{-/-}$ mice backcrossed onto the C57BL/6 background ($n > 9$) were originally obtained from GalPharma Co., Ltd. and are described elsewhere (Seki et al., 2008). Mice bred at the La Jolla Institute for Allergy and Immunology and WT mice were used as controls where required. All experiments reported here were approved by the La Jolla Institute for Allergy and Immunology Animal Care Committee and are in compliance with the animal care and use guidelines of the Association for the Assessment and Accreditation of Laboratory Animal Care and the National Institutes of Health.

Antibodies and flow cytometric analysis. Agonist anti–4-1BB (clone 3H3, isotype rat IgG2a) was previously described (Shuford et al., 1997) and produced and purified from a hybridoma. Rat IgG2a was purchased from Sigma-Aldrich. The following antibodies were used for flow cytometry: PE-conjugated anti–Gal-9 (108A2) and anti-CD25 (PC61), PE-Cy7–conjugated anti-NK1.1 (PK136) and anti–IFN-γ (XMG1.2), FITC-conjugated anti-CD44 and anti-CD49b (DX5), peridinin chlorophyll protein–conjugated CD62L (MEL-14), peridinin chlorophyll protein–Cy5.5-conjugated CD8β and anti–L-17A, Pacific blue–conjugated anti-CD3ε (145-2C11) and anti-CD4 (GK1.5), biotin-conjugated anti–4-1BB and anti-OX40, allophycocyanin-conjugated anti–Gr-1 (RB6-8C5), anti–rat IgG (Poly4054), and streptavidin (all from BioLegend); PE-conjugated anti–4-1BBL (TKS-1) and anti–Gal-3 (M3/38), Alexa Flour 700–conjugated MHC class II (M5/114.15.2), and FITC-conjugated anti-CD11c (N418; all from eBioscience). PE-conjugated anti–Siglec-F (E5-2440) was from BD.

Intracellular staining was performed after lysing RBCs, and draining LN cells were plated in round-bottom, 96-well microtiter plates in 200 µl with 200 µg/ml $MOG_{33–55}$ peptide for 72 h at 37°C, and 8 h before harvesting, GolgiPlug (BD) was added. Cells were preincubated with 10 µg/ml anti–mouse CD16/CD32 (2.4G2) to block FcγR and stained with Pacific blue anti-CD4, fixed with Cytofix/Cytoperm (BD), and then stained with PerCP-Cy5.5 anti–IL-17A and PE-Cy7 anti–IFN-γ. Samples were analyzed after gating on CD4$^+$ T cells on an LSR-II flow cytometer (BD) and FlowJo software (Tree Star). In other experiments, cells were stimulated for 6 h with 50 ng/ml PMA and 500 ng/ml ionomycin in the presence of GolgiPlug (BD). Cells were preincubated with anti–mouse CD16/CD32 and stained for Pacific blue–, PercP-Cy5.5–, or FITC-conjugated mAb against mouse CD3ε, CD8β, and CD11c surface molecules, respectively. Cells were fixed and made permeable with a Cytofix/Cytoperm Plus kit (BD) and stained with PE-Cy7–conjugated anti–IFN-γ. Samples were analyzed after gating on CD3$^+$CD8β$^+$ T cells on an LSR-II flow cytometer and FlowJo software.

BAL cells were preincubated with anti–mouse CD16/CD32 and then stained with PE-conjugated Siglec-F, FITC-conjugated CD11c, and APC-conjugated Gr-1 for 30 min. BAL cells were washed with FACS buffer, and eosinophils were identified as the Siglec-F$^+$CD11c$^-$ population. Samples were analyzed on a LSR-II flow cytometer and FlowJo software. The absolute numbers of each population were calculated by multiplying the percentage measured by flow cytometry by the total number of viable cells (absolute number = percentage × total cells recovered).

Cloning, production, and purification of Fc fusion proteins. 4-1BB cDNA was amplified by reverse transcription using total RNA of activated splenic CD4 T cells from C57BL/6 mice. cDNA for mouse full-length extracellular 4-1BB (CRD1–4 and transmembrane regions, amino acids 24–187) and truncated mutants of 4-1BB extracellular domains (CRD1–2, 24–85; CRD2–3, 46–117; CRD3–4 and transmembrane, 86–187; and CRD4 and transmembrane, 118–187), containing either the N-terminal signal sequence of 4-1BB or IL-2, was inserted into the PS1121 human IgG1 Fc (Hinge-CH2-CH3) backbone (a gift from C. Benedict, La Jolla Institute for Allergy and Immunology, La Jolla, CA) flanked with HindIII and EcoRI restriction enzyme sites. For human 4-1BB.Fc, 4-1BB cDNA was obtained by RT-PCR using total RNA of activated PBMCs (cryopreserved from ZenBio). cDNA for full-length extracellular 4-1BB (CRD1-4 and transmembrane regions, amino acids 24–186) and each truncated form of 4-1BB (CRD1–3, 24–118; and CRD4 and transmembrane, 119–186) was ligated into the PS1121 huIgG1 Fc vector. For 4-1BBL.Fc, mouse 4-1BBL cDNA was obtained from total RNA of LPS-activated splenic CD11c$^+$ DCs by RT-PCR. The entire ectodomain of 4-1BBL (amino acids 104–309) was inserted into the PS1121 huIgG1 Fc vector using HindIII and EcoRI sites. The sequences of each construct were confirmed by DNA sequencing at Retrogen, Inc. All Fc fusion proteins were expressed using Freestyle HEK 293F expression system (Invitrogen) according to supplier's protocol and purified by protein G affinity chromatography. For some experiments, Fc proteins were made in HEK 293S cells (GnTI$^-$) or HEK 293T cells using calcium phosphate transfection.

Production of C- and N-terminal Gal-9. Full-length mouse Gal-9 cDNA and recombinant human and mouse Gal-9 proteins were *Escherichia coli* derived and a gift of GalPharma Co., Ltd. Mouse C-terminal (amino acids 1–188) and N-terminal (amino acids 216–353) Gal-9 were expressed using the pGEX-4T2 expression system (GE Healthcare) in *E. coli* BL21 (DE3) and purified as previously reported (Bulliard et al., 2013).

Binding assays. For plate-based binding assays, mouse Gal-1 (R&D Systems), Gal-9 (GalPharma Co., Ltd.), or 4-1BBL (R&D Systems) was coated onto ELISA plates, and binding of various Fc fusion proteins was detected using anti-Fc HRP by reading the optical density at 450 nm. For flow cytometry–based assays, protein G beads (Invitrogen) were coated with saturating amounts of mouse 4-1BB.Fc or control Fc fusion protein, and binding of mouse Galectins or 4-1BBL was detected using fluorescent antibodies. For competition experiments, mouse 4-1BB.Fc–coated beads were first incubated with either mouse 4-1BBL or Gal-9, washed, and incubated with either mouse Gal-9 or 4-1BBL, respectively, and binding of these proteins was detected using fluorescent antibodies. In some experiments, mouse 4-1BB.Fc–coated beads were first incubated with anti–4-1BB (clones 3H3 or 1D8), washed, and incubated with mouse Gal-9. For precipitation-based assays, full-length or mutant human and mouse 4-1BB.Fc proteins were coated on to the beads and incubated with human or mouse Gal-9 (GalPharma Co., Ltd.), Gal-4 (R&D Systems), or 4-1BBL (R&D Systems). In some experiments, mouse Gal-9 mutants containing either C- or N-terminal domains were used. Coprecipitation was detected by SDS-PAGE (reducing condition) by eluting the proteins from the beads. Individual proteins were run in different lanes to identify corresponding bands in the experimental lanes. Human and mouse Gal-9 and Gal-4 were *E. coli* derived with predicted and observed molecular masses of ∼36 kD. Human 4-1BBL was also *E. coli* derived with predicted and observed molecular masses of ∼20 kD. Mouse 4-1BBL was mouse myeloma cell line derived with predicted and observed molecular masses of 26 and 41–44 kD, respectively, on SDS-PAGE with reducing conditions (as per manufacturer-supplied information; R&D Systems).

SPR measurements. A Biacore3000 instrument (GE Healthcare) was used to determine human and mouse Gal-9 equilibrium binding affinity.

Anti–human IgGs (human antibody capture kit; GE Healthcare) were amine coupled to a CM5 sensor chip using the amine coupling kit according to the manufacturer's instructions (GE Healthcare). Human and mouse 4-1BB.Fc (full-length or CRD4 mutant variant) were diluted in running buffer (10 mM Hepes, pH 7.4, 150 mM NaCl, 3 mM EDTA, 0.005% Tween 20), and ∼500 response units (RU) were immobilized on the sensor chip. A human IgG (Fc fragment) or irrelevant Fc fusion protein was used as a negative control for nonspecific binding. Human or mouse Gal-9 was diluted in SPR running buffer and passed over the immobilized sensor chip at 25°C with a flow rate of 30 µl/min using increasing concentrations of Gal-9 (00.004–0.312 µM). Kinetic parameters were calculated using a simple Langmuir 1:1 model with the BIA evaluation software version 4.1. For domain binding of Gal-9, mutants of human and mouse 4-1BB.Fc (full-length or mutant variants) were diluted in running buffer and immobilized to get ∼500 RU. A human IgG (Fc fragment) or irrelevant Fc fusion protein was used as a negative control for nonspecific binding. A single concentration (2.5 µM) of human or mouse Gal-9 was diluted in SPR running buffer and passed over the immobilized sensor chip at 25°C with a flow rate of 30 µl/min. For carbohydrate-mediated binding studies, mouse or human CRD4 4-1BB.Fc was either control treated or treated with PNGase F/Endo H enzymes (New England Biolabs, Inc.) as suggested. 2.5 µM mouse or human Gal-9 was injected over immobilized CRD4 4-1BB.Fc (untreated and deglycosylated). A human IgG (Fc fragment) protein was used as a negative control for nonspecific binding and used for reference subtraction.

Immunofluorescent microscopy. 2×10^5 cells were immobilized on poly-L-lysine–coated glass coverslips (BD) for 30 min, fixed with 4% paraformaldehyde (PFA)/PBS (GE Healthcare) for 15 min, and permeabilized with 0.3% saponin/PBS for 5 min. After blocking with 5% BSA/PBS, rat anti–mouse 4-1BB 3E1 clone (Shuford et al., 1997) and rabbit anti–mouse Gal-9 (Novus Biologicals) antibodies were treated at room temperature for 1 h, followed by anti–rat IgG–Alexa Fluor 555 (Cell Signaling Technology) and anti–rabbit IgG–Alexa Fluor 488 (Invitrogen), with three PBS washing steps in between. After treatment with DAPI for 10 min, for visualizing the nuclei, cells were mounted with FluorSave Reagent (EMD Millipore). Immunofluorescence was analyzed at ×60 with an Axiovert 200M microscope (Carl Zeiss) integrated with Intelligent Imaging Innovations SlideBook 4.2 software.

Immunoprecipitations, SDS-PAGE, and Western blotting. FACS-purified naive CD4 T cells or NK cells were preactivated for 2 d with anti-CD3/CD28 or IL-2, respectively. In some experiments, 4-1BB$^{-/-}$ T hybridoma cells were generated from activated 4-1BB$^{-/-}$ CD4 T cells fused with BW5147 thymoma cells. These 4-1BB$^{-/-}$ T cell hybridomas transduced either with full-length (FL; 1–256 aa) or cytoplasmic deletion mutant (ΔC; 1–213 aa) of 4-1BB were used. Cells were either restimulated or left untreated, and 10^7 cells were lysed in 1 ml of 1% NP-40 lysis buffer (20 mM Tris-Cl, pH 7.4, 150 mM NaCl, 2 mM EDTA, 1% NP-40, 10% glycerol, and 50 mM NaF) supplemented with a protease inhibitor cocktail and PhosSTOP (Roche) for 30 min with 100 passages through a 23-gauge needle on a 3-ml syringe, on ice. Lysates were centrifuged at 4K rpm for 15 min. After removal of insoluble precipitates, clear lysates were incubated with 4-1BBL.Fc fusion protein bound to protein G Dynabeads (Invitrogen) at 4°C overnight. After several washes with NP-40 lysis buffer, proteins were eluted from the beads in glycine-HCl (0.1 M, pH 2.6) and prepared for gel electrophoresis in LDS sample buffer (Invitrogen) with 0.1 M DTT. Samples were loaded onto 10% or 4–12% NuPAGE Bis-Tris precast gels (Invitrogen). After SDS-PAGE, the proteins were transferred onto polyvinylidene fluoride membranes (Invitrogen) for Western blotting with rat anti–mouse 4-1BB (EMD Millipore) or rat anti–mouse Gal-9 (BioLegend), followed by anti–rat IgG light chain–specific HRP (Jackson ImmunoResearch Laboratories, Inc.). All blots were developed with Immobilon Western HRP substrate (EMD Millipore). For nuclear and cytosolic separation in NF-κB assay, NE-PER Nuclear and Cytoplasmic Extraction Reagent (Thermo Fisher Scientific) was used, and equal loading and purity of nuclear contents were verified by assessing Lamin B (C-20; Santa Cruz Biotechnology, Inc.). Anti-RelA rabbit pAb (C-20) was used for NF-κB nuclear translocation.

DC isolation and RALDH induction. Spleens were pretreated with collagen (Sigma-Aldrich) for 30 min at 37°C. Single cell suspensions were incubated with anti–mouse CD11c microbeads (Miltenyi Biotec) and positively selected on MACS columns. Cells were further purified by cell sorting by gating on CD11c$^+$MHC II^{hi}. DCs were cultured with 500 pg/ml GM-CSF for 48 h. These cells were resorted for identical expression of 4-1BB, and $2–3 \times 10^5$ DCs were further cultured with 2.5 µg/ml zymosan in the presence of 5 µg/ml control rat IgG (KLH/G1-2-2) or 5 µg/ml anti–4-1BB (3H3) for another 24 h. The activity of RALDH was determined by the ALDEFLUOR staining kit (STEMCELL Technologies).

In vitro T and NK cell culture. CD4$^+$ and CD8$^+$ splenic T cells were pre-enriched with CD4 and CD8 microbeads (Miltenyi Biotec), respectively. Naive CD4 and CD8 T cells were further purified by cell sorting by gating cells as CD25$^-$CD44^{lo}CD62L^{hi}. Naive T cells were preactivated with 2 µg/ml of plate-bound anti-CD3 (2C11) and 0.5 µg/ml of soluble anti-CD28 (37N5) for 48 h. To determine secondary responsiveness, these activated/effector T cells were resorted for identical expression of 4-1BB and recultured with 0.5 µg/ml of plate-bound anti-CD3 in the presence of 10 µg/ml of control rat IgG or 10 µg/ml anti–4-1BB (3H3) without any APCs for another 24 h. In some experiments, effector CD8 T cells were recultured with varying concentrations of recombinant mouse 4-1BBL (his-tagged and cross-linked with anti-polyhistidine antibody; R&D Systems) or irradiated 4-1BBL$^+$ hybridoma cells in the presence of 10 µg/ml of control rat IgG or a blocking anti–4-1BBL (19H3; 10 µg/ml) for another 48 h. Culture supernatants were collected and cytokines measured by ELISA with antibodies to IL-2 (JES6-1A12 and biotin-JES6-5H4) and IFN-γ (R46A2 and biotin-XMG1.2; all from BD).

Splenic NK cells were pre-enriched by MACS with CD49b (DX5) microbeads. NK cells were further purified by cell sorting by gating on CD3$^-$DX5$^+$. Sorted NK cells were preactivated with 50 ng/ml recombinant IL-2 (PeproTech) for 72 h. These NK cells were resorted for identical expression of 4-1BB and recultured with varying concentrations of anti-NK1.1 (PK136) or anti–4-1BB (3H3) or recombinant mouse 4-1BBL (cross-linked with anti-polyhistidine antibody) or control rat IgG in the presence of 20 ng/ml recombinant IL-2 for another 48 h. Culture supernatants were collected and ELISA performed with antibodies to IFN-γ (R46A2 and biotin-XMG1.2; all from BD).

Induction of EAE. 8-wk-old female mice were immunized by s.c. injection at the base of the tail with 100 µg $MOG_{33–55}$ peptide (AnaSpec) emulsified in an equal volume of CFA (Life Technologies) containing 2 mg/ml *Mycobacterium tuberculosis* H37 RA (Difco) on day 0. The mice also received i.v. injections of 200 ng pertussis toxin (List Biological Laboratories) on days 0 and 2 and were administered i.p. 100 µg anti–4-1BB (clone 3H3) or control antibody (rat IgG) on days 0, 2, 4, and 8. Individual animals were scored daily for clinical signs of EAE using the following criteria: 0, no detectable signs of disease; 0.5, distal limp tail; 1, complete limp tail; 1.5, limp tail and hind limb weakness; 2, unilateral partial hind paralysis; 2.5, bilateral partial hind limb paralysis; 3, complete bilateral hind limb paralysis; 3.5, complete bilateral hind limb paralysis and unilateral forelimb; 4, total paralysis of fore and hind limbs; and 5, death.

Induction of allergic airway inflammation. WT and Gal-9$^{-/-}$ mice were immunized with 20 µg OVA (Sigma-Aldrich) adsorbed to 2 mg aluminum hydroxide and magnesium hydroxide (Alum; Thermo Fischer Scientific) i.p. on days 1 and 14, followed by 20 µg OVA in 20 µl PBS given intranasally on days 14–16. 200 µg anti–4-1BB (clone 3H3) or 200 µg control antibody (rat IgG) was injected i.p. 1 d before the first OVA immunization. Mice were sacrificed on day 18, and BAL fluid, lungs, and lung-draining LNs were obtained. For collection of BAL fluid, tracheas were cannulated, and the lungs were lavaged six times with 800 µl PBS (2% BSA). Cells in the

lavage fluid were counted, and BAL cell differentials were determined using flow cytometry based on cell surface markers. Lung-draining LN cells from antigen-induced mice were isolated and restimulated (2×10^6 cells per ml) in vitro with 100 µg/ml OVA in culture medium for 72 h. Cultures were pulsed with 0.25 µCi [^{3}H]TdR thymidine for the final 14 h, and activity was measured in a scintillation counter (Wallac MicroBeta TriLux; PerkinElmer). Simultaneously culture supernatants were collected, and IFN-γ and IL-5 were measured by ELISA (BD).

Histological analysis. Mice were anesthetized with sodium pentobarbital and intracardially perfused through the right ventricle with ice-cold PBS. Spinal cords from EAE-induced mice were dissected, fixed in 4% PFA (Electron Microscopy Sciences), and paraffin embedded, and 6-µm sections were stained with H&E. Lungs from asthma-induced mice were perfused with 4% PFA, dissected, fixed in 4% PFA, and paraffin embedded, and 6-µm sections were stained with H&E for visualization of inflammatory infiltrates. To ensure comparable analyses between different groups, six to eight randomly selected sections were analyzed per animal. For inflammation scoring in lungs, peribronchial regions (six to eight per mouse) were evaluated at 200×, and inflammatory infiltrates around the airways were graded for severity (0, normal; 1, <3-cell-diameter thick; 2, 3–10 cells thick; 3, >10 cells thick) and extent (0, normal; 1, <10% of sample; 2, 10–25%; 3, >25%). Scores were calculated by multiplying severity by extent (max 9).

Statistics. Two-tailed Student's *t* test was used to determine the statistical significance of differences between groups using Prism 6.0 (GraphPad Software). P-values of <0.05 were considered statistically significant.

Online supplemental material. Fig. S1 shows proposed models of how Gal-9 might mediate 4-1BB oligomerization after interaction with 4-1BBL or anti–4-1BB and control 4-1BB signaling. Online supplemental material is available at http://www.jem.org/cgi/content/full/jem.20132687/DC1.

This work was supported by National Institutes of Health grants AI042944 and AI089624 to M. Croft. This is manuscript 1666 from the La Jolla Institute for Allergy and Immunology.

T. Niki and M. Hirashima are board members of GalPharma Co., Ltd. Although there are patents and products in development, this does not alter the authors' adherence to all of the journal policies on sharing data and materials, as detailed in the guide for authors.

Author contributions: S. Madireddi, S.-Y. Eun, S.-W. Lee, and M. Croft conceived of the project; S. Madireddi and I. Nemčovičová performed and analyzed SPR data; S. Madireddi and S.-W. Lee performed and analyzed binding data; S.-Y. Eun designed and cloned Fc fusion, FL 4-1BB, ΔC 4-1BB, and 4-1BBL constructs and generated T hybridoma cell clones expressing each protein, and S. Madireddi produced Fc fusion proteins; S.-Y. Eun performed confocal microscopy, and S.-Y. Eun and S. Madireddi analyzed the data. S.-Y. Eun performed and analyzed immunoprecipitation and Western blotting experiments; S. Madireddi generated and analyzed the in vitro functional data and EAE data; S. Madireddi and A.K. Mehta generated and analyzed airway inflammation data; A.K. Mehta analyzed histology data; D.M. Zajonc and S.-W. Lee provided intellectual input and experimental advice; D.M. Zajonc, N. Nishi, T. Niki, and M. Hirashima contributed reagents and contributed to the preparation of the manuscript; and S. Madireddi and M. Croft wrote the manuscript.

Submitted: 26 December 2013
Accepted: 16 May 2014

REFERENCES

Arikawa, T., K. Watanabe, M. Seki, A. Matsukawa, S. Oomizu, K.M. Sakata, A. Sakata, M. Ueno, N. Saita, T. Niki, et al. 2009. Galectin-9 ameliorates immune complex-induced arthritis by regulating FcγR expression on macrophages. *Clin. Immunol.* 133:382–392. http://dx.doi.org/10.1016/j.clim.2009.09.004

Ascierto, P.A., E. Simeone, M. Sznol, Y.X. Fu, and I. Melero. 2010. Clinical experiences with anti-CD137 and anti-PD1 therapeutic antibodies. *Semin. Oncol.* 37:508–516. http://dx.doi.org/10.1053/j.seminoncol.2010.09.008

Bi, S., P.W. Hong, B. Lee, and L.G. Baum. 2011. Galectin-9 binding to cell surface protein disulfide isomerase regulates the redox environment to enhance T-cell migration and HIV entry. *Proc. Natl. Acad. Sci. USA.* 108:10650–10655. http://dx.doi.org/10.1073/pnas.1017954108

Bodmer, J.L., P. Schneider, and J. Tschopp. 2002. The molecular architecture of the TNF superfamily. *Trends Biochem. Sci.* 27:19–26. http://dx.doi.org/10.1016/S0968-0004(01)01995-8

Bossen, C., K. Ingold, A. Tardivel, J.L. Bodmer, O. Gaide, S. Hertig, C. Ambrose, J. Tschopp, and P. Schneider. 2006. Interactions of tumor necrosis factor (TNF) and TNF receptor family members in the mouse and human. *J. Biol. Chem.* 281:13964–13971. http://dx.doi.org/10.1074/jbc.M601553200

Bulliard, Y., R. Jolicoeur, M. Windman, S.M. Rue, S. Ettenberg, D.A. Knee, N.S. Wilson, G. Dranoff, and J.L. Brogdon. 2013. Activating Fc γ receptors contribute to the antitumor activities of immunoregulatory receptor-targeting antibodies. *J. Exp. Med.* 210:1685–1693. http://dx.doi.org/10.1084/jem.20130573

Chan, F.K. 2007. Three is better than one: Pre-ligand receptor assembly in the regulation of TNF receptor signaling. *Cytokine.* 37:101–107. http://dx.doi.org/10.1016/j.cyto.2007.03.005

Chan, F.K., H.J. Chun, L. Zheng, R.M. Siegel, K.L. Bui, and M.J. Lenardo. 2000. A domain in TNF receptors that mediates ligand-independent receptor assembly and signaling. *Science.* 288:2351–2354. http://dx.doi.org/10.1126/science.288.5475.2351

Chattopadhyay, K., U.A. Ramagopal, A. Mukhopadhaya, V.N. Malashkevich, T.P. Dilorenzo, M. Brenowitz, S.G. Nathenson, and S.C. Almo. 2007. Assembly and structural properties of glucocorticoid-induced TNF receptor ligand: Implications for function. *Proc. Natl. Acad. Sci. USA.* 104:19452–19457. http://dx.doi.org/10.1073/pnas.0709264104

Chattopadhyay, K., E. Lazar-Molnar, Q. Yan, R. Rubinstein, C. Zhan, V. Vigdorovich, U.A. Ramagopal, J. Bonanno, S.G. Nathenson, and S.C. Almo. 2009. Sequence, structure, function, immunity: structural genomics of costimulation. *Immunol. Rev.* 229:356–386. http://dx.doi.org/10.1111/j.1600-065X.2009.00778.x

Choi, B.K., T. Asai, D.S. Vinay, Y.H. Kim, and B.S. Kwon. 2006. 4-1BB-mediated amelioration of experimental autoimmune uveoretinitis is caused by indoleamine 2,3-dioxygenase-dependent mechanisms. *Cytokine.* 34:233–242. http://dx.doi.org/10.1016/j.cyto.2006.04.008

Chou, F.C., S.J. Shieh, and H.K. Sytwu. 2009. Attenuation of Th1 response through galectin-9 and T-cell Ig mucin 3 interaction inhibits autoimmune diabetes in NOD mice. *Eur. J. Immunol.* 39:2403–2411. http://dx.doi.org/10.1002/eji.200839177

Compaan, D.M., and S.G. Hymowitz. 2006. The crystal structure of the costimulatory OX40-OX40L complex. *Structure.* 14:1321–1330. http://dx.doi.org/10.1016/j.str.2006.06.015

Croft, M., C.A. Benedict, and C.F. Ware. 2013. Clinical targeting of the TNF and TNFR superfamilies. *Nat. Rev. Drug Discov.* 12:147–168. http://dx.doi.org/10.1038/nrd3930

Earl, L.A., S. Bi, and L.G. Baum. 2011. Galectin multimerization and lattice formation are regulated by linker region structure. *Glycobiology.* 21:6–12. http://dx.doi.org/10.1093/glycob/cwq144

Foell, J., S. Strahotin, S.P. O'Neil, M.M. McCausland, C. Suwyn, M. Haber, P.N. Chander, A.S. Bapat, X.J. Yan, N. Chiorazzi, et al. 2003. CD137 costimulatory T cell receptor engagement reverses acute disease in lupus-prone NZB × NZW F_1 mice. *J. Clin. Invest.* 111:1505–1518. http://dx.doi.org/10.1172/JCI200317662

Fulcher, J.A., M.H. Chang, S. Wang, T. Almazan, S.T. Hashimi, A.U. Eriksson, X. Wen, M. Pang, L.G. Baum, R.R. Singh, and B. Lee. 2009. Galectin-1 co-clusters CD43/CD45 on dendritic cells and induces cell activation and migration through Syk and protein kinase C signaling. *J. Biol. Chem.* 284:26860–26870. http://dx.doi.org/10.1074/jbc.M109.037507

Golden-Mason, L., R.H. McMahan, M. Strong, R. Reisdorph, S. Mahaffey, B.E. Palmer, L. Cheng, C. Kulesza, M. Hirashima, T. Niki, and H.R. Rosen. 2013. Galectin-9 functionally impairs natural killer cells in humans and mice. *J. Virol.* 87:4835–4845. http://dx.doi.org/10.1128/JVI.01085-12

Grigorian, A., S. Torossian, and M. Demetriou. 2009. T-cell growth, cell surface organization, and the galectin-glycoprotein lattice. *Immunol. Rev.* 230:232–246. http://dx.doi.org/10.1111/j.1600-065X.2009.00796.x

Hirabayashi, J., T. Hashidate, Y. Arata, N. Nishi, T. Nakamura, M. Hirashima, T. Urashima, T. Oka, M. Futai, W.E. Muller, et al. 2002. Oligosaccharide specificity of galectins: a search by frontal affinity chromatography. *Biochim. Biophys. Acta.* 1572:232–254. http://dx.doi.org/10.1016/S0304-4165(02)00311-2

Katoh, S., N. Ishii, A. Nobumoto, K. Takeshita, S.Y. Dai, R. Shinonaga, T. Niki, N. Nishi, A. Tominaga, A. Yamauchi, and M. Hirashima. 2007. Galectin-9 inhibits CD44-hyaluronan interaction and suppresses a murine model of allergic asthma. *Am. J. Respir. Crit. Care Med.* 176:27–35.

Kim, Y.H., B.K. Choi, S.M. Shin, C.H. Kim, H.S. Oh, S.H. Park, D.G. Lee, M.J. Lee, K.H. Kim, D.S. Vinay, and B.S. Kwon. 2011. 4-1BB triggering ameliorates experimental autoimmune encephalomyelitis by modulating the balance between Th17 and regulatory T cells. *J. Immunol.* 187:1120–1128. http://dx.doi.org/10.4049/jimmunol.1002681

Kwon, B.S., and S.M. Weissman. 1989. cDNA sequences of two inducible T-cell genes. *Proc. Natl. Acad. Sci. USA.* 86:1963–1967. http://dx.doi.org/10.1073/pnas.86.6.1963

Kwon, B.S., C.A. Kozak, K.K. Kim, and R.T. Pickard. 1994. Genomic organization and chromosomal localization of the T-cell antigen 4-1BB. *J. Immunol.* 152:2256–2262.

Lee, S.W., and M. Croft. 2009. 4-1BB as a therapeutic target for human disease. *Adv. Exp. Med. Biol.* 647:120–129. http://dx.doi.org/10.1007/978-0-387-89520-8_8

Lee, S.W., Y. Park, S.Y. Eun, S. Madireddi, H. Cheroutre, and M. Croft. 2012. Cutting edge: 4-1BB controls regulatory activity in dendritic cells through promoting optimal expression of retinal dehydrogenase. *J. Immunol.* 189:2697–2701. http://dx.doi.org/10.4049/jimmunol.1201248

Loo, D.T., N.J. Chalupny, J. Bajorath, W.W. Shuford, R.S. Mittler, and A. Aruffo. 1997. Analysis of 4-1BBL and laminin binding to murine 4-1BB, a member of the tumor necrosis factor receptor superfamily, and comparison with human 4-1BB. *J. Biol. Chem.* 272:6448–6456. http://dx.doi.org/10.1074/jbc.272.10.6448

Matsumoto, R., H. Matsumoto, M. Seki, M. Hata, Y. Asano, S. Kanegasaki, R.L. Stevens, and M. Hirashima. 1998. Human ecalectin, a variant of human galectin-9, is a novel eosinophil chemoattractant produced by T lymphocytes. *J. Biol. Chem.* 273:16976–16984. http://dx.doi.org/10.1074/jbc.273.27.16976

Nagae, M., N. Nishi, T. Murata, T. Usui, T. Nakamura, S. Wakatsuki, and R. Kato. 2006. Crystal structure of the galectin-9 N-terminal carbohydrate recognition domain from Mus musculus reveals the basic mechanism of carbohydrate recognition. *J. Biol. Chem.* 281:35884–35893. http://dx.doi.org/10.1074/jbc.M606648200

Naismith, J.H., and S.R. Sprang. 1998. Modularity in the TNF-receptor family. *Trends Biochem. Sci.* 23:74–79. http://dx.doi.org/10.1016/S0968-0004(97)01164-X

Nonaka, Y., T. Ogawa, S. Oomizu, S. Nakakita, N. Nishi, S. Kamitori, M. Hirashima, and T. Nakamura. 2013. Self-association of the galectin-9 C-terminal domain via the opposite surface of the sugar-binding site. *J. Biochem.* 153:463–471. http://dx.doi.org/10.1093/jb/mvt009

Ohtsubo, K., S. Takamatsu, M.T. Minowa, A. Yoshida, M. Takeuchi, and J.D. Marth. 2005. Dietary and genetic control of glucose transporter 2 glycosylation promotes insulin secretion in suppressing diabetes. *Cell.* 123:1307–1321. http://dx.doi.org/10.1016/j.cell.2005.09.041

Oomizu, S., T. Arikawa, T. Niki, T. Kadowaki, M. Ueno, N. Nishi, A. Yamauchi, and M. Hirashima. 2012. Galectin-9 suppresses Th17 cell development in an IL-2-dependent but Tim-3-independent manner. *Clin. Immunol.* 143:51–58. http://dx.doi.org/10.1016/j.clim.2012.01.004

Pace, K.E., C. Lee, P.L. Stewart, and L.G. Baum. 1999. Restricted receptor segregation into membrane microdomains occurs on human T cells during apoptosis induced by galectin-1. *J. Immunol.* 163:3801–3811.

Polte, T., J. Foell, C. Werner, H.G. Hoymann, A. Braun, S. Burdach, R.S. Mittler, and G. Hansen. 2006. CD137-mediated immunotherapy for allergic asthma. *J. Clin. Invest.* 116:1025–1036. http://dx.doi.org/10.1172/JCI23792

Rabinovich, G.A., and M.A. Toscano. 2009. Turning 'sweet' on immunity: galectin-glycan interactions in immune tolerance and inflammation. *Nat. Rev. Immunol.* 9:338–352. http://dx.doi.org/10.1038/nri2536

Rabinovich, G.A., M.A. Toscano, S.S. Jackson, and G.R. Vasta. 2007. Functions of cell surface galectin-glycoprotein lattices. *Curr. Opin. Struct. Biol.* 17:513–520. http://dx.doi.org/10.1016/j.sbi.2007.09.002

Rabu, C., A. Quéméner, Y. Jacques, K. Echasserieau, P. Vusio, and F. Lang. 2005. Production of recombinant human trimeric CD137L (4-1BBL). Cross-linking is essential to its T cell co-stimulation activity. *J. Biol. Chem.* 280:41472–41481. http://dx.doi.org/10.1074/jbc.M506881200

Salek-Ardakani, S., and M. Croft. 2010. Tumor necrosis factor receptor/tumor necrosis factor family members in antiviral CD8 T-cell immunity. *J. Interferon Cytokine Res.* 30:205–218. http://dx.doi.org/10.1089/jir.2010.0026

Sato, M., N. Nishi, H. Shoji, M. Seki, T. Hashidate, J. Hirabayashi, K. Kasai Ki, Y. Hata, S. Suzuki, M. Hirashima, and T. Nakamura. 2002. Functional analysis of the carbohydrate recognition domains and a linker peptide of galectin-9 as to eosinophil chemoattractant activity. *Glycobiology.* 12:191–197. http://dx.doi.org/10.1093/glycob/12.3.191

Schabowsky, R.H., K.G. Elpek, S. Madireddi, R.K. Sharma, E.S. Yolcu, L. Bandura-Morgan, R. Miller, K.J. MacLeod, R.S. Mittler, and H. Shirwan. 2009. A novel form of 4-1BBL has better immunomodulatory activity than an agonistic anti-4-1BB Ab without Ab-associated severe toxicity. *Vaccine.* 28:512–522. http://dx.doi.org/10.1016/j.vaccine.2009.09.127

Seki, M., K.M. Sakata, S. Oomizu, T. Arikawa, A. Sakata, M. Ueno, A. Nobumoto, T. Niki, N. Saita, K. Ito, et al. 2007. Beneficial effect of galectin 9 on rheumatoid arthritis by induction of apoptosis of synovial fibroblasts. *Arthritis Rheum.* 56:3968–3976. http://dx.doi.org/10.1002/art.23076

Seki, M., S. Oomizu, K.M. Sakata, A. Sakata, T. Arikawa, K. Watanabe, K. Ito, K. Takeshita, T. Niki, N. Saita, et al. 2008. Galectin-9 suppresses the generation of Th17, promotes the induction of regulatory T cells, and regulates experimental autoimmune arthritis. *Clin. Immunol.* 127:78–88. http://dx.doi.org/10.1016/j.clim.2008.01.006

Seo, S.K., J.H. Choi, Y.H. Kim, W.J. Kang, H.Y. Park, J.H. Suh, B.K. Choi, D.S. Vinay, and B.S. Kwon. 2004. 4-1BB-mediated immunotherapy of rheumatoid arthritis. *Nat. Med.* 10:1088–1094. http://dx.doi.org/10.1038/nm1107

Shuford, W.W., K. Klussman, D.D. Tritchler, D.T. Loo, J. Chalupny, A.W. Siadak, T.J. Brown, J. Emswiler, H. Raecho, C.P. Larsen, et al. 1997. 4-1BB costimulatory signals preferentially induce $CD8^+$ T cell proliferation and lead to the amplification in vivo of cytotoxic T cell responses. *J. Exp. Med.* 186:47–55. http://dx.doi.org/10.1084/jem.186.1.47

Siegel, R.M., J.K. Frederiksen, D.A. Zacharias, F.K. Chan, M. Johnson, D. Lynch, R.Y. Tsien, and M.J. Lenardo. 2000. Fas preassociation required for apoptosis signaling and dominant inhibition by pathogenic mutations. *Science.* 288:2354–2357. http://dx.doi.org/10.1126/science.288.5475.2354

Snell, L.M., G.H. Lin, A.J. McPherson, T.J. Moraes, and T.H. Watts. 2011. T-cell intrinsic effects of GITR and 4-1BB during viral infection and cancer immunotherapy. *Immunol. Rev.* 244:197–217. http://dx.doi.org/10.1111/j.1600-065X.2011.01063.x

So, T., S.W. Lee, and M. Croft. 2008. Immune regulation and control of regulatory T cells by OX40 and 4-1BB. *Cytokine Growth Factor Rev.* 19:253–262. http://dx.doi.org/10.1016/j.cytogfr.2008.04.003

Su, E.W., S. Bi, and L.P. Kane. 2011. Galectin-9 regulates T helper cell function independently of Tim-3. *Glycobiology.* 21:1258–1265. http://dx.doi.org/10.1093/glycob/cwq214

Sun, Y., X. Lin, H.M. Chen, Q. Wu, S.K. Subudhi, L. Chen, and Y.X. Fu. 2002. Administration of agonistic anti-4-1BB monoclonal antibody leads to the amelioration of experimental autoimmune encephalomyelitis. *J. Immunol.* 168:1457–1465. http://dx.doi.org/10.4049/jimmunol.168.3.1457

Türeci, O., H. Schmitt, N. Fadle, M. Pfreundschuh, and U. Sahin. 1997. Molecular definition of a novel human galectin which is immunogenic in patients with Hodgkin's disease. *J. Biol. Chem.* 272:6416–6422. http://dx.doi.org/10.1074/jbc.272.10.6416

Vaitaitis, G.M., and D.H. Wagner Jr. 2012. Galectin-9 controls CD40 signaling through a Tim-3 independent mechanism and redirects the cytokine profile of pathogenic T cells in autoimmunity. *PLoS ONE.* 7:e38708. http://dx.doi.org/10.1371/journal.pone.0038708

Vinay, D.S., and B.S. Kwon. 2012. Immunotherapy of cancer with 4-1BB. *Mol. Cancer Ther.* 11:1062–1070. http://dx.doi.org/10.1158/1535-7163.MCT-11-0677

Watts, T.H. 2005. TNF/TNFR family members in costimulation of T cell responses. *Annu. Rev. Immunol.* 23:23–68. http://dx.doi.org/10.1146/annurev.immunol.23.021704.115839

Wiersma, V.R., M. de Bruyn, W. Helfrich, and E. Bremer. 2013. Therapeutic potential of Galectin-9 in human disease. *Med. Res. Rev.* 33:E102–E126. http://dx.doi.org/10.1002/med.20249

Wilson, N.S., B. Yang, A. Yang, S. Loeser, S. Marsters, D. Lawrence, Y. Li, R. Pitti, K. Totpal, S. Yee, et al. 2011. An Fcγ receptor-dependent mechanism drives antibody-mediated target-receptor signaling in cancer cells. *Cancer Cell*. 19:101–113. http://dx.doi.org/10.1016/j.ccr.2010.11.012

Won, E.Y., K. Cha, J.S. Byun, D.U. Kim, S. Shin, B. Ahn, Y.H. Kim, A.J. Rice, T. Walz, B.S. Kwon, and H.S. Cho. 2010. The structure of the trimer of human 4-1BB ligand is unique among members of the tumor necrosis factor superfamily. *J. Biol. Chem*. 285:9202–9210. http://dx.doi.org/10.1074/jbc.M109.084442

Zhou, Z., X. Song, A. Berezov, G. Zhang, Y. Li, H. Zhang, R. Murali, B. Li, and M.I. Greene. 2008. Human glucocorticoid-induced TNF receptor ligand regulates its signaling activity through multiple oligomerization states. *Proc. Natl. Acad. Sci. USA*. 105:5465–5470. http://dx.doi.org/10.1073/pnas.0711350105

Zhu, C., A.C. Anderson, A. Schubart, H. Xiong, J. Imitola, S.J. Khoury, X.X. Zheng, T.B. Strom, and V.K. Kuchroo. 2005. The Tim-3 ligand galectin-9 negatively regulates T helper type 1 immunity. *Nat. Immunol*. 6:1245–1252. http://dx.doi.org/10.1038/ni1271